2018

Use Of Induced Pluripotent Stem Cell Models To Elucidate Retinal Disease Pathogenesis And To Develop Gene-Based Therapies

Thu Thi Duong
University of Pennsylvania, thuduong2011@gmail.com

Use Of Induced Pluripotent Stem Cell Models To Elucidate Retinal Disease Pathogenesis And To Develop Gene-Based Therapies

Abstract
Choroideremia (CHM) is a rare monogenic, X-linked recessive inherited retinal degenerative disease caused by mutations in the Rab Escort Protein-1 (REP1) encoding CHM gene. CHM is characterized by childhood-onset night blindness (nyctalopia), progressive peripheral vision loss due to the degeneration of neural retina, RPE and choroid in a peripheral-to-central fashion. Most of CHM mutations are loss-of-function mutations leading to the complete lacking of REP1 protein. However, the primary retinal cell type leading to CHM and molecular mechanism remains unknown in addition to the fact of lacking proper disease models. In this study, we explored the utility of induced pluripotent stem cell-derived models of retinal pigment epithelium (iPSC-RPE) to study disease pathogenesis and a potential gene-based intervention in four different genetically distinct forms of CHM. A number of abnormal cell biologic, biochemical, and physiologic functions were identified in the CHM patient cells. Transduction efficiency testing using 11 recombinant adeno-associated virus (AAV) serotype 1-9, 7m8 and 8b showed a differential cell tropism on iPSC and iPSC-derived RPE. We identified AAV7m8 to be optimal for both delivering transgenes to iPSC-RPEs as well as to appropriate target cells (RPE cells and rod photoreceptors) in the primate retina. To establish the proof of concept of AAV7m8 mediated CHM gene therapy, we developed a AAV7m8.hCHM viral vector, which delivers the human CHM cDNA under control of CMV-enhanced chicken β-actin promoter (CβA). Delivery of AAV7m8.CMV.CβA.hCHM to CHM iPSC-RPEs restored protein prenylation, trafficking and phagocytosis defects. The results confirm that AAV-mediated delivery of the REP1-encoding gene can rescue defects in CHM iPSC-RPE regardless of the type of disease-causing mutation. The results also extend our understanding of mechanisms involved in the pathophysiology of choroideremia.

Degree Type
Dissertation

Degree Name
Doctor of Philosophy (PhD)

Graduate Group
Cell & Molecular Biology

First Advisor
Jean Bennett

Keywords
CHM, choroideremia, gene augmentation, induced pluripotent stem cells, in vitro models, REP1

Subject Categories
Molecular Biology

USE OF INDUCED PLURIPOTENT STEM CELL MODELS TO ELUCIDATE RETINAL DISEASE PATHOGENESIS AND TO DEVELOP GENE-BASED THERAPIES

Thu Thi Duong

A DISSERTATION

in

Cell and Molecular Biology

Presented to the Faculties of the University of Pennsylvania

in

Partial Fulfillment of the Requirements for the

Degree of Doctor of Philosophy

2018

Supervisor of Dissertation

_____

Dr. Jean Bennett, M.D., Ph.D.
Professor of Ophthalmology, F.M. Kirby Center for Molecular Ophthalmology, Center for Advanced Retinal and Ocular Therapeutics (CAROT), Scheie Eye Institute, University of Pennsylvania Perelman School of Medicine

Graduate Group Chairperson

_____

Dr. Daniel S. Kessler, Ph.D.
Associate Professor of Cell and Developmental Biology, University of Pennsylvania Perelman School of Medicine

Dissertation Committee

Dr. Nancy A. Speck, Ph.D., Professor of Cell and Developmental Biology, University of Pennsylvania Perelman School of Medicine

Dr. Katherine A. High, M.D., Professor of Pediatrics, Children's Hospital of Philadelphia

Dr. Joshua L. Dunaief, M.D, Ph.D., Professor of Ophthalmology, University of Pennsylvania Perelman School of Medicine

Dr. Paul J. Gadue, Ph.D., Associate Professor of Pathology and Laboratory Medicine, University of Pennsylvania Perelman School of Medicine

ACKNOWLEDGMENT

I do not think I could have come this far in my academic endeavors if it were not for the encouragement, inspiration, and support of so many people I have met in my life.

I was born in an extended family with five other siblings in a rural area of North Vietnam where I witnessed the difficulties in terms of limited finances as well as poor living conditions that my parents have been through. My mom, Đặng Thị Yến, only finished her fourth grade, but she was a smart and creative retailer with a modern mindset. She took care of all of us when my father worked in the South of Vietnam and could only visit us one or twice a year. She sent my oldest sister to study English afterschool in the only school that taught English which was located far away from our village. When we moved to the South of Vietnam, my mom invited an English teacher to come to our house to teach us English at home. My mom is the one who inspired me that English is the language that can change my life in a lot of ways. My father, Dương Thanh Trước, was a diligent hardworking worker in an oil rig firm. This is a tough manual labor job with a strange working schedule that messed up his biological clock. When my father was home, he did everything with my mom and he repaired all broken things to make them usable again. He was so good to us and wanted us to have the best, so he wore old clothes to save the new clothes for sale. He cooked and washed our clothes to save us time and money for studying. My father also had to study English to be able to work with foreign colleagues, but in his time, he was too poor to be able to afford white paper. He used the brown paper cover of cement bags collected from construction sites to write in all four directions of the paper until there was no more empty space to write. Life could be so difficult for my

parents, but they gave us the privilege to get a proper education. My parents are my endless inspiration who encouraged me to be aware that education can foster me to reach a new horizon. Con cảm ơn Bố Mẹ! In addition, I would like to express my appreciation to my oldest sister, Ms. Thuy Duong, for all of her investment in my education, her belief in me, her support and her care to me when I was in college.

My destiny with biomedical sciences started with a journey full of new knowledge outside of the textbook I learned from my high school Biology teacher, Mrs. Thuỷ, in preparation for the national competition. Despite my parents wanting me to become a doctor or a pharmacist, Mrs. Thuỷ showed me the beauty of this life science subject and encouraged me to study biotechnology as she emphasized this is going to be one of the frontier technologies in the 21st century. I chose to pursue the bachelor degree in Biotechnology at the University of Science in Ho Chi Minh City, Vietnam from 2004 - 2008. It was there that I was exposed to many different aspects of biotechnology and fell in love with Cell and Molecular Biology, Assisted Reproductive Technology, especially Stem cell research, thanks to many inspiring teachers. Thầy Phan Kim Ngọc (head of Laboratory of Stem cell research and application) is one of the most inspiring teachers I met there. His laboratory was the place which nurtured my naïve love with stem cell research. Despite all of the limitations and difficulties, e.g. lack of equipment – only one culture hood for all staff and students, lack of financial support – we recycled everything we could e.g. washing plastic p1000, p200 pipet tips and autoclaved them to re-use, lack of mentors – new graduates like me carried out research on our own and mentored last year college students, I was still excited to do my work and kept my dream to study abroad in the near future. I recall a thrilling feeling when Nhung, a last year college student, and I first successfully cloned the *PDX1* gene from original vector, a gift from a Vietnamese's professor in Australia, to the other expression vector by traditional restriction enzyme

method. It took us a few months to do a procedure which can be done in a few days. We sang and danced in the lab after seeing the PDX1 band cutting from the expression plasmid in the agarose gel! I will never forget the day, the people, and the place where I began my baby steps into science.

For a scholarship hunter like me, encouragement from receiving financial support for my study played an important role in my academic achievement. Thanks to many scholarships from University of Science to help cover my tuition, from Japan's UFJ Foundation and one week summer school program in Tsukuba University in Japan have led me to my dream of studying aboard in the United States. The Vietnam Education Foundation (www.vef.gov) awarded a fellowship and a letter of recommendation from two prestigious American professors for me to apply for graduate school in the U.S. This is a great opportunity for me not only to experience myself in an outstanding academic environment in the U.S., getting extra-training in many more skills e.g. leadership and public narrative, but also extend my network with more than 500 Vietnamese fellows and scholars in many different fields of STEM to do a lot of projects that benefit Vietnam. Without VEF, I would have never dreamed of getting accepted to the University of Pennsylvania for my Ph.D. training.

I think my admission committee, Dr. Sarah Millar, Dr. Peter S. Klein and my department coordinator, Mrs. Meagan Schofer, could not forget a Vietnamese student who proactively asked for an opportunity to be interviewed. Looking back I cannot believe I was able to be so proactive and aggressive with obtaining an interview after applying, but my drive to be at UPenn and work in stem cell and regenerative medicine field pushed me. It was that determination that made me reach out directly to the committee because I could not let this opportunity slip away. When I came to the U.S. in Fall 2011, I found so many challenges and difficulties adapting to the most amazing yet competitive academic

environment at UPenn. Not only the language barrier, but also the in-depth knowledge I was lacking, caused me at many times to doubt my capabilities in getting my graduate degree. But my department chairs, Dr. Sarah Millar and Dr. Stephen DiNardo, and my mentor, Dr. Jean Bennett have been and continue to be amazingly supportive and encouraging.

Every professor I met at UPenn is a source of inspiration and encouragement. I remember the day Dr. Sarah Millar called me into her office after knowing my bad grade on the second exam of the Cell 600 course to look for a way to help me overcome the difficulties. She found me a tutor for Cell 600. Later, Sarah and Steve asked my Developmental, Stem Cells and Regenerative Biology department to pay for my English writing course in the summer. In my second year of grad school, Jean and Steve discussed my research proposal with me many times to boost my confidence in presenting it on the white board in front of my preliminary exam committee. I remember very clearly the image of Dr. Peter Klein showing me how to design my own primers for the first time during my second lab rotation in his lab. Dr. Nancy Speck and Dr. Stephen DiNardo explained to me the requirements of “CAMB first year seminar course” and motivated me to raise my hand and discuss science with my classmates.

I have a long way to go in my academic endeavor to deserve your trust. But I know you would be happy to hear that the opportunity you all gave me, I have paid it forward to many more Vietnamese students and children, by organizing the VEFFA mentoring program to assist Vietnamese students to prepare for their graduate school applications and the Vietnam Book Drive to send donated research books and English children’s books from the U.S. to Vietnam. Thank you all so much for believing in me!

I would like to express my most gratitude to Dr. Jean Bennett, Dr. Vidyullatha Vasireddy, Dr. Jeannette Bennicelli, and Dr. Jason A. Mills.

I came to do my third rotation in Dr. Jean Bennett's Lab in the end of my first year of grad school at UPenn. In my first email to ask for a lab rotation in Dr. Bennett's Lab, I mentioned my cousin, Mr. Khải Đặng, who is becoming a blind person due to a childhood accident. He was instrumental in my decision to focus on treatments for the blind in order to help him and his friends in their struggle. I did not know that pursuing my goals and this destiny would allow me to meet the most amazing mentor in the world! I admire Jean in a lot of ways for her dedication, inspiration, her optimism, and her great leadership. She is my role model professionally and personally. I want to become a translational scientist like you. Without you, the first FDA approved gene therapy inherited retinal degeneration could not go to the market and help people. I want to become a mentor like you who has a strength and inspiration that can resolve and relieve any burden and worry from the new trainees. I am so fortunate to have an opportunity to work with you. I have experienced the most interesting and meaningful stage of my life in the past six years being your trainee. You walked me through many obstacles to fulfill the requirements of my Ph.D. training, you supported me to apply for HHMI fellowship after going through the internal nomination and AAUW woman's fellowship, you were generous to allow me have time with my family during my visit, you were wonderful to allow me a week to fly to UC Davis to help my friend who got trouble in her mental health due to losing her mom. I cannot thank you enough. I love you and I am forever grateful for your support. Thank you so much, Dr. Bennett and all the members of Bennett's Lab who have been so friendly and supportive to me over the last years.

Dr. Vidyullatha Vasireddy was the first person I worked with in Bennett's Lab. Latha understood me amazingly well and gave me instructions in everything I need for my experiments. I can discuss everything with her academically and personally. I thank you so much for being my mentor and my best friend.

Dr. Jeannette Bennicelli contributed a great effort in the establishment of the stem cell core in Bennett's Lab. I have learned many great things from her in doing different research projects. Thank you, Jeannette!

Dr. Jason A. Mills joined Bennett's lab recently as a faculty and a director of stem cell core. Since then, I have been working with him so efficiently and quickly in the past one year with choroideremia patient derived *in vitro* cellular models. I have never seen a talented person with a quick mind full of ideas and creative approaches like you. You played a very important role in the scientific development and experimental designs for my two recent publications. I thank you so much for your guidance and support.

I would like to send my great appreciation to my thesis committee, Dr. Nancy A. Speck, Dr. Katherine A. High, Dr. Joshua L. Dunaief, and Dr. Paul J. Gadue for your time, commitment and support. I could not imagine that my committee spent time and shared their wisdom with my mentor to discuss the best way for me to develop my career and tackle my immigration obstacle when I decided to change my intention and stay in the U.S longer. I am so touched, honored and grateful to be your student!

Last but not least, I would like to send my appreciation to all of my friends who have been become a part of my life journey. Thank you, my lifelong best friends - my siblings, Chị Thuỷ, Chị Thanh, Thái, Ngọc and Lộc for everything. Thank you, my best friends – Minh Nguyệt and Bích Ngọc – for being my best friends. Thank you, Hayley Hanby, for being my amazing classmate and great friend in the Ph.D. training at UPenn. Thank you, Adam, Teddy, Vicki, Niki, Leo, Pam, Marisa, Lindsey, Devin, Scott, Laura, Aaron, Jen, Ivan, Wei, Tyler for being my amazing labmates. Thank you, all of my friends who used to live or has been living in house 4039 for supporting me. Thank you all of my VEFFA friends for working with me in a lot of meaningful projects and consulting me in different aspects of science. Thank you, all of my American friends, who helped me to run

the Vietnam Book Drive project at PennMOVES and Annual Book Day at UPenn. And, thank you, my English tutor, Nathan who provides comedy during my stressful times.

I am so fortunate to have the most amazing mentors, teachers, trainers and friends in my life. Thank you all for everything!

Sincerely,

Thu Thi Duong

ABSTRACT

USE OF INDUCED PLURIPOTENT STEM CELL MODELS TO ELUCIDATE RETINAL DISEASE PATHOGENESIS AND TO DEVELOP GENE-BASED THERAPIES

Thu Thi Duong

Jean Bennett

Choroideremia (CHM) is a rare monogenic, X-linked recessive inherited retinal degenerative disease caused by mutations in the Rab Escort Protein-1 (REP1) encoding *CHM* gene. CHM is characterized by childhood-onset night blindness (nyctalopia), progressive peripheral vision loss due to the degeneration of neural retina, RPE and choroid in a peripheral-to-central fashion. Most of *CHM* mutations are loss-of-function mutations leading to the complete lacking of REP1 protein. However, the primary retinal cell type leading to CHM and molecular mechanism remains unknown in addition to the fact of lacking proper disease models. In this study, we explored the utility of induced pluripotent stem cell-derived models of retinal pigment epithelium (iPSC-RPE) to study disease pathogenesis and a potential gene-based intervention in four different genetically distinct forms of CHM. A number of abnormal cell biologic, biochemical, and physiologic functions were identified in the CHM patient cells. Transduction efficiency testing using 11 recombinant adeno-associated virus (AAV) serotype 1-9, 7m8 and 8b showed a differential cell tropism on iPSC and iPSC-derived RPE. We identified AAV7m8 to be optimal for both delivering transgenes to iPSC-RPEs as well as to appropriate target cells (RPE cells and rod photoreceptors) in the primate retina. To establish the proof of concept of AAV7m8 mediated CHM gene therapy, we developed a AAV7m8.hCHM viral vector, which delivers the human *CHM* cDNA under control of CMV-enhanced chicken β-actin promoter (CβA). Delivery of AAV7m8.CMV.CβA.hCHM to CHM iPSC-RPEs restored

protein prenylation, trafficking and phagocytosis defects. The results confirm that AAV-mediated delivery of the REP1-encoding gene can rescue defects in CHM iPSC-RPE regardless of the type of disease-causing mutation. The results also extend our understanding of mechanisms involved in the pathophysiology of choroideremia.

Table of Contents

LIST OF TABLES

LIST OF FIGURES

CHAPTER 1 - INTRODUCTION

RETINA AND RETINAL DISEASES

Retina: structure, function and its diseases

The retina is located in the posterior chamber of the eye and is comprised of multiple layers of cells functioning to gather light photons, turning them into neuronal signals, then transmitting the signals to the visual cortex of the brain to create our vision. The stratified neural retina contains, photoreceptor, amacrine, bipolar, horizontal, ganglion, and Müller cells, and the neural retina is anterior and adjacent to the retinal pigment epithelium (RPE) cell monolayer. Rod photoreceptors are responsible for dim light vision whereas cone photoreceptors, including S-cones, M-cones and L-cones, are sensitive to short-wavelength, medium-wavelength and long-wavelength light, respectively and are thus responsible for color vision. In humans or non-human primates, the macular region, in the center of the retina, has a foveal region which is concentrated with cone photoreceptors. This structure relays visual acuity. Retinal pigment epithelium resides adjacent to the photoreceptor layers and plays a significant role in visual function and photoreceptor maintenance including: 1) light absorption; 2) reisomerization of all-trans-retinal into 11-cis-retinal for the visual cycle; 3) transport of nutrients, ions, and water between photoreceptors and the choriocapillaris; 4) phagocytosis of photoreceptor outer segment for their continuous regeneration; and 5) secretion of trophic factors for the integrity of the retina and choriocapillaris (Simó et al., 2010).

There are many different non-syndromic and syndromic retinal diseases leading to irreversible blindness. They can be either dominant, recessive or X-linked disease, for example mutations in *RPE65* which has an important role in reisomerization of all-trans-retinal into 11-cis-retinal on retinoid cycle, can cause Leber Congenital Amaurosis 2 (LCA2) (Cai et al., 2009). In another example, loss of function mutations in the *CHM* gene located on the X chromosome can cause Choroideremia (M. Preising and Ayuso, 2004). In terms of inherited retinal degeneration, there are more than 200 causative genes currently identified (Siemiatkowska et al., 2014). Mutations in any of those genes can alter the normal function of the retina at the molecular to physical level, causing degeneration of photoreceptors or RPE.

Models to study retinal degenerative pathogenesis

To recapitulate human retinal diseases, there are several available model systems for study. Zebrafish provide an excellent model for studying ocular development because they are phylogenetically similar to human (70% of human genes are found in zebrafish), easy to genetically manipulation, they propagate regularly due to a short life cycle, their transparent embryos provide a useful tool for imaging and protein tracking during development, and maintenance requirements for zebrafish are minimal (Ail and Perron, 2017; Link and Collery, 2015). Murine models are very popular for studies of human retinal diseases and development because of the similarity in anatomy and physiology. The growing toolbox for genetic and epigenetic modifications makes conditional and knockout mice very accessible for studies of various cellular and molecular pathways associated with pathogenesis of the disease. For ophthalmologic studies, the accessibility of the eye for non-invasive studies such as analyses of cellular structure and topography using optical coherence tomography (OCT), fundus imaging, and analyses of retinal function

using electroretinograms (ERGs) make animal models great resources for investigation (Veleri et al., 2015). Due to differences in the shorter life span of mice (1 years old mice = 30 years old human in term of development), characterization of disease phenotypes and study of developmental biology can be expedited in murine models (Veleri et al., 2015). A challenge for murine models is that mice are nocturnal. They have an enrichment of rod (compared to cone) photoreceptors (unlike human) and do not have macula, a region responsible for color vision and visual acuity. Hence, in some diseases especially macular degeneration, murine models are not ideal. In many instances, the murine model does not recapitulate the human disease; therefore, providing a knockout or conditional genetic manipulation is not always useful. Non-human primate (NHP) models are the closest in term of genetic and functional similarity to humans and the presence of a macula is a major advantage for translational studies (Mustari, 2017). However, there are multiple factors making NHPs challenging model to study, e.g. the limited number of animals that can be studied, the ethical issues, the difficulties of genetic modification, the lack of disease models in NHPs, and the high expense of maintaining the large animal models (Mustari, 2017). Since the discovery of embryonic stem cells (ESC) and induced pluripotent stem cells (iPSC), patient derived cellular models harboring precise mutations of each patient facilitate scientific elucidation of disease pathogenesis. Pluripotent stem cells provide a tool to study the early development of the retina as they create a means for investigating all three germ layers; endoderm, mesoderm, and ectodermal tissues. Recently, a significant amount of effort has been put into developing highly efficient and sophisticated strategies to generate retinal cell subtypes in two-dimensional or three-dimensional cultures (Nakano et al., 2012; David A. Parfitt et al., 2016; Sonoda et al., 2009; Zhong et al., 2014). Given the capacity of iPSCs to recapitulate embryonic

development, these cells have been able to replace embryonic stem cells eliminating the ethical issues with human ESCs.

CHOROIDEREMIA

Choroideremia (CHM) is an X-linked recessive chorioretinal dystrophy characterized by the degeneration of retinal photoreceptor cells, retinal pigment epithelium (RPE) and choroid. The onset of clinical symptoms in CHM, is typically observed within the first or second decade of life. Early symptoms observed are poor night vision and a progressive loss of peripheral vision. As the disease progresses, there is a loss of central vision leading to eventual complete blindness. The latter can be observed by the fifth decade of life. (Aleman et al., 2017; Sanchez-Alcudia et al., 2016) The disease typically affects only males, while females are carriers of the disease. The prevalence of CHM is about 1:50,000, hence it is considered a rare disease. Disease mechanisms are believed to be molecularly and biochemically explained by the lack of Rab Escort Protein 1 (REP1) function due to loss-of-function mutations in the REP1-encoding *CHM* gene. This results in loss of posttranslational lipid modification of ras-related GTPases, or Rab proteins (prenylation of Rab proteins). The defect in prenylation disrupts intracellular trafficking of vesicles, motility and fusion of organelles in cells, specifically retinal cells (RPE, Photoreceptors). However, the primary cell type(s) causing the degeneration is still not clearly identified. Currently, there are no established treatments for CHM; however, there are two early phase AAV mediated gene therapy clinical trials for CHM that were initiated several years ago and are on-going (Nightstar Therapeutics, 2018a; Spark Therapeutics, 2018) and plans for a phase 3 trial (Nightstar Therapeutics, 2018b).

CHM pathophysiology

CHM is an X-linked disease, so it affects hemizygous males. Patients with choroideremia experience night blindness in the first or second decade of life, followed by progressive peripheral vision loss. This leads to tunnel vision which ultimately encroaches on the fovea and often leads to complete blindness in the fourth to fifth decades of life. Fovea region which determines central vision is the last area that was observed to be affected in CHM. Fundus images show a progressive atrophy of the choriocapillaris and RPE which expands in a peripheral to central fashion (M. Preising and Ayuso, 2004). This pattern suggests a secondary degeneration of photoreceptors due to primary and progressive RPE atrophy. Histopathology studies on a deceased eye from a 30-year-old male with choroideremia caused by a nonsense mutation, revealed an independent degeneration of all affected cell types affected in CHM, including choriocapillaris, RPE, and photoreceptors (MacDonald et al., 2009). The clinical profile at any given age and between the two eyes of affected subjects with choroideremia can be variable suggesting that, although CHM is a single gene defect, other factors may play a role in moderating the final disease phenotype. The heterozygous carrier females do not develop a visual impairment, but may have signs of patchy chorioretinal degeneration due to random X-chromosome inactivation (Heckenlively and Bird, 1988).

CHM mutations

The *CHM* gene (OMIM:300390) is comprised of 15 exons and spans over 180 kb of Xq21.2. The coding sequence of *CHM* is 1.9 kb and the gene encodes a 653 amino acid protein, REP-1. There are more than 300 mutation variants that have been identified in the *CHM* gene in individuals with choroideremia and these mutations can affect any

region of the gene. These mutations include nonsense, missense mutations, splicing defects, small and large insertions and deletions (Simunovic et al., 2016). There is a small group of CHM patients in whom mutations were not identified. Overall, the majority of causative mutations of CHM are loss-of-function mutations leading to the absence of REP1 protein physically and functionally. In addition, there are a couple of missense mutations in *CHM* that have been reported. A novel *CHM* missense variant (c.1520A>G; p.H507R) was discovered to be associated with the disease in Italian CHM patients (Esposito et al., 2011). This missense mutation does not cause any difference in mRNA and DNA level, but creates a lesser amount of functional REP1 protein than found in unaffected individuals. In addition, the REP1 protein in such patients is unable to associate with RabGGTase for a normal prenylation cycle (Esposito et al., 2011). Another missense variant in CHM is c. 1679T>C (p. L550P) which may cause the instability of native folded REP1 protein due to a mutation-caused lack of a hydrogen bond between the two beta strands (Sergeev et al., 2009). *CHM* mutations were observed to be located in both coding and non-coding regions of CHM. A recent publication investigated the potential for variants in the *CHM* promoter region (c.-98: C>A and C>T), to segregate with the disease (Radziwon et al., 2017). An effort to study the correlation of genotype and phenotype in a cohort of 74 CHM patients with mutations ranging from insertions, to deletions, splicing defects, and single point mutations in which majority were null mutations indicated no clear relationship in terms of the effects of the mutations on visual acuity, visual field, residual retina area, age of onset (Simunovic et al., 2016).

Function of REP1 protein

The REP-1 protein is ubiquitously expressed in the body. It plays an important role in the prenyl (geranylgeranyl) post-translational modification of Rab GTPases (Rab),

members of the Ras superfamily of monomeric G proteins. A vast variety of Rab proteins has been identified so far. All these Rabs, when integrated in membranes, are involved in protein trafficking, docking and membrane tethering. Before integration of Rabs into membranes, they must be post-translationally modified through the addition of two prenyl groups to 1-2 cysteines located near the C-terminus of the Rab protein (Pylypenko et al., 2003; Seabra et al., 1995, 1992; Strunnikova et al., 2009). This geranylgeranyl post-translational modification is called prenylation. In the cytosol, REP1 will present newly synthesized, unprenylated hydrophilic Rab proteins to a catalytic Rab geranylgeranyltransferase (GGTase) in order to add geranylgeranyl group into Cysteine residues on the C-terminus. Then the prenylated Rabs are escorted to their specific destination membrane (Pylypenko et al., 2003), a fundamental process for intracellular vesicular transport in endocytic and exocytic pathways.

An accumulation of unprenylated Rab proteins in the cytosol is an indication of the lack of REP1 characterizing CHM patients. Even though REP1 protein is observed to be completely absent in CHM patients, the disease phenotype is specific to the ocular tissue, indicating the retina-specific role of REP1. The lack of other symptoms in patients with choroideremia is due to compensation by a redundant autosomal homologue of *CHM, CHML*, choroideremia-like protein (REP2), is located on chromosome 1q42 (Cremers et al., 1994). REP2 has an additional three amino acids and is encoded by just one single exon. However, it is 75% identical to REP1. Due to these similarities, REP2 compensates for the function of REP1 in non-ocular tissues. The affinity of REP1 with Rabs is higher compared to REP2 (Köhnke et al., 2013; Rak et al., 2004).

The addition of a prenyl group will tether the Rab proteins to the membrane associated with the trafficking of related proteins (M. N. Preising and Ayuso, 2004). There

are more than 70 types of Rab proteins. Choroideremia could be due to a deficiency of prenylation in multiple Rab proteins, for example, Rab27a, Rab6, and/or Rab8. In the photoreceptor, the intracellular trafficking of proteins from the inner segment to the outer segment, rhodopsin for example, occurs via the budding of vesicles from the Golgi apparatus to the connecting cilium. This is regulated by Rab8 and Rab6 (Deretic, 1998). In the RPE, intracellular trafficking by Rab27a protein in combination with myosin VIIA controls the phagocytosis and degradation of photoreceptor outer segments via the transport of the phagosome (Gibbs et al., 2003). In retinal tissue, loss of REP1 can affect the trafficking of opsin from the cell body to outer segment regions, or the migration of melanosomes to the apical region, as well as the rate of phagocytosis of photoreceptor outer segments by the RPE.

Recent studies of a cohort of 9 patients with *CHM* mutations revealed systemic findings such as prominent crystals in lymphocytes and significant fatty acid abnormalities (Zhang et al., 2015a) suggesting that molecular mechanism of CHM is may extend to other cell types.

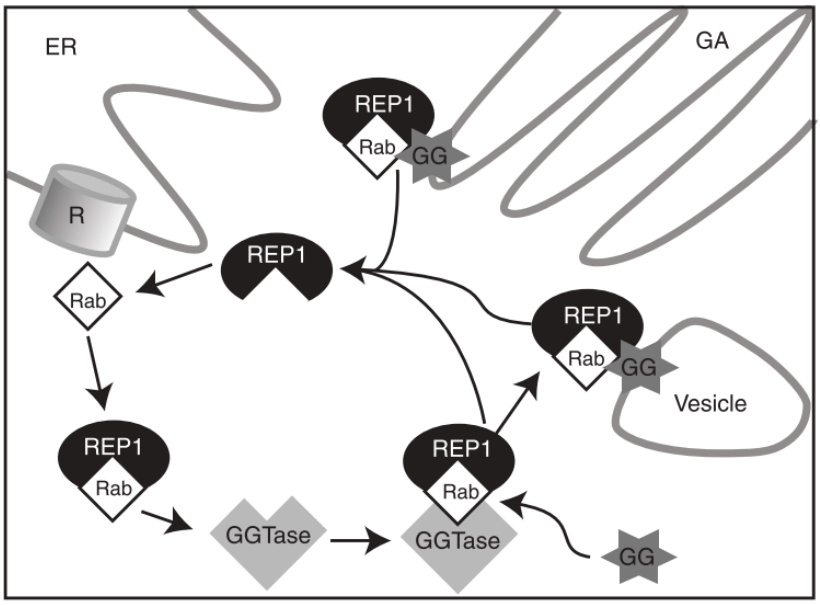

Figure 1. A schematic of the cellular function of Rab escort protein (REP1).

REP1 presents newly synthesized, unprenylated Rabs to a catalytic Rab geranylgeranyltransferase (GGTase) subunit in order to add one or more hydrophobic prenyl groups (geranylgeranyl, GG shown here) to carboxy-terminal cysteine residues (a process called prenylation). Prenylated Rabs have as their characteristics, the ability to target particular membranes in the Golgi apparatus (GA) and of diverse cellular vesicles (Vesicle, represents various cellular vesicles, e.g., lysosomes or transport vesicles) (Alun R. Barnard, Markus Groppe, 2015).

Disease models

The pathophysiological mechanism of CHM is complex and not yet clearly known. RPE and photoreceptors have a tight inter-connected relationship which suggests that if either cell layer degenerates, that will lead to a secondary degeneration of the other. Identification of the primary cell type causing the disease would pave the way in developing gene augmentation therapy targeting the appropriate affected cells. To understand more about the pathophysiology of the disease, various animal models were developed.

Zebrafish CHM model

In 2007, Krock et al. reported a degeneration of RPE and photoreceptors in 4.5 days post fertilization *chm* nonsense mutant fish. Studies of the mosaic model suggested that defective RPE cells failed to phagocytize outer segments of photoreceptors thereby leading to secondary degeneration of the photoreceptors (Krock et al., 2007). In fact, disease in the *chm (-/-)* zebrafish manifests as an extremely severe systemic illness resulting in early lethality at day 5 to day 6 post fertilization (Moosajee et al., 2009). This severe lethality is explained by the lack of redundancy of other isoforms of REP1 (e.g. REP2 in mammalian) in this common non-mammalian vertebrate model organism. This severe phenotype limits the application of zebrafish model in studying human CHM disease.

Murine CHM model

Chm knock-out in mice is embryonically lethal. Complete loss of REP1 in hemizygous males and heterozygous females caused embryonic death when the gene was transmitted from heterozygous females (Van den Hurk et al., 1997). This might

indicate the difference in function of REP1 in mice compared to humans. The cell type specific conditional knockout mouse model has been created to study the independent role(s) of photoreceptors and RPE relative to the disease manifestation (Tolmachova et al., 2010). Loss of REP1 in photoreceptors of these mice resulted in a slowly progressive photoreceptors degeneration while the RPE layer maintains to be healthy with normal pigmentation and melanosome distribution. Loss of REP1 in RPE cells only was not observed to alter the integrity of photoreceptors layer, but shown to affect the pigmentation of RPE in some areas and the distribution of melanosomes in RPE. Further evaluation of the RPE specific REP1 ablation in mice showed a decrease of melanosomes in the apical side and a delay in phagosome degradation (Silène T. Wavre-Shapton et al., 2013). In these mice, melanosomes were observed to be localized in the cell body, leading to decreased melanosomes in the apical area of the RPE. In the mouse model where REP1 was absent in both RPE and photoreceptors, acceleration of photoreceptors degeneration was reported only in young mice. This study revealed that either photoreceptors or RPE can be the primary cell type that leads in CHM disease. However, none of these models were successful in mimicking a human CHM disease phenotype. The major hurdles in developing any therapeutic strategies for monogenic disease are the failure to establish the molecular mechanism underlying the disease progression or the lack of suitable animal model to test the therapy. In CHM, the challenge is that the genetically modified animal model does not closely resemble the functional and morphologic characteristics of the human CHM disease with complete accuracy. Moreover, the engineered models are not readily available. Therefore, it is important to focus studies on developing *in vitro* cell based methods to understand the pathophysiology of the disease and to test the therapeutic approach. For these reasons, human derived cell types from induced

pluripotent stem cells are considered as promising models to study this CHM pathogenesis.

In vitro cellular models

Development of therapeutic interventions in certain retinal degenerative diseases is hampered by the lack of relevant models of the diseases. As the current research on human subjects, particularly for therapeutic interventions for retinal diseases, is limited by ethical guidelines, establishment of surrogate models that accurately recapitulate disease phenotypes is necessary. These cell-based models could enable the efficient translation of basic research so that it could ultimately then be applied in the clinical setting. Potential *in vitro* models would include primary retinal photoreceptors or RPE cells that are specific to patients. But obtaining these cells as a biopsy from living human retina would be harmful to the patient. The recent advancement of induced pluripotent stem cell (iPSC) and embryonic stem cell (ESC)-derived cells could technically establish an *in vitro* model system to study CHM.

As shown in CHM murine model, photoreceptors and RPE have an independent effect on CHM disease pathogenesis. Taking advantage of induced pluripotent stem cell technology, patient derived cellular model may serve as personalized models to explore the disease mechanism. In the retina, photoreceptors directly connect with RPE and get support from RPE to perform their visual function in term of structure integrity, trophic factors secretion, nutrient exchange, visual cycle, outer segment phagocytosis (Sparrow et al., 2010; Strauss, 2005).

The photoreceptor cell is not an easy cell type to culture for research purpose. Scientific evidence shows that photoreceptors quickly lose their structural integrity when cultured. Studies using an *in vitro* co-culturing system with RPE cells were carried out to

try to overcome this, but still, culturing of photoreceptors was not successful. Generating 3D retinal eyecups is a recent advancement aiming to develop a structure resembling the mature retinal tissue (Zhong et al., 2014) with an achievement of a few outer segments in those optic vesicles. However, the ability to generate fully mature photoreceptors still has a long way to go and it is a real challenge (Zhong et al., 2014).

Compared to the culture of photoreceptors, culture of retinal pigment epithelium (RPE) *in vitro* has been shown to result in maintenance of the RPE fundamental characteristics. Fetal RPE was cultured and developed a thin, confluent cell layer with pigmented hexagon morphology with the expression of all RPE markers as measured at transcriptional and translational levels (the early eye field development marker, PAX6; the RPE-specific transcription factors MITF and OTX2; the tight junction marker, ZO-1, N-cadherin; the secreted, PEDF, VEGF; the membrane-associated proteins, BEST1; the visual cycle proteins, RPE65, LRAT, CRALBP; the pre-melanosome protein (PMEL17) (Sonoda et al., 2009; Zhang et al., 2012). RPE was cultured in apical or basal surfaces, melanosome transport to apical side, as the establishment of tight junction between cells as measured by high transepithelial resistance (TER) (Sonoda et al., 2009). Patient derived RPE from human embryonic stem cells or induced pluripotent stem cells has been generated over the last decade to serve the purpose of modeling *in vivo* RPE. Improving from a spontaneous differentiation protocol to a direct differentiation using a combination of retinal inducing factors (IGF1, Noggin, Dkk1, and bFGF) and other factors (nicotinamide, Activin A, SU5402, and VIP), efficiency of *in vitro* RPE differentiation increased from a small portion of cells to 80% population that has Pmel17 expression (pre-melanosome protein) (Buchholz et al., 2009; Uchholz et al., 2013).

iPSC and iPSC derived RPE were used as tools to study CHM disease mechanisms by two different groups (Cereso et al., 2014; Vasireddy et al., 2013). iPS cells

generated by CHM patients showed the lack of function of REP1 proteins. Both studies delivered the functional REP1 using adeno-associated virus and tested the ability to restore REP1 function in personalized *in vitro* models of CHM.

Gene augmentation therapy

Since the molecular mechanism behind choroideremia is the loss of functional REP1, delivering functional REP1 protein to the retina could protect the retina from degenerative changes. Targeting the monogenic disease caused by mutations is usually based on gene correction or gene augmentation. Rather than correcting the nonfunctional gene, gene augmentation therapy serves as a superior strategy, where a functional copy of the deficient gene will be delivered to the cells that are affected by loss of the specific gene. Gene augmentation was reported to work well for recessive diseases where there is a complete lack of functional protein. Delivery of functional genes/proteins can be achieved by both non-viral and viral mediated approach. Non-viral mediated gene delivery is focused on delivering the functional gene without using any viral vectors. The advantage of using this strategy is a) less immunological response due to the viral capsids; 2) the ability to package larger genes. Even though this strategy is less toxic, several challenges including low efficacy and transient expression still need to be addressed.

On the other hand, viral mediated gene augmentation therapy uses recombinant viral vectors to deliver transgenes. A variety of recombinant viral vectors, like retrovirus, lentivirus, adenovirus, is available that can deliver the transgene to specific cell types. Due to the safety and efficacy profile of recombinant adeno-associated virus (AAV) in animals and humans, this viral vector has become a useful tool in several degenerative diseases, including retinal degeneration. Recombinant adeno-associated viruses are currently the most favorable viral vectors for gene augmentation therapy due to their low

immunogenicity, toxicity; lack of genome integration; and the ability to transduce both dividing and quiescent cells in a stable fashion.

Adeno-associated virus (AAV)

Adeno-associated virus has opened a new chapter for gene therapy after a long challenging time dealing with immunogenicity of adenovirus or lentivirus. Adeno-associated virus (AAV) is a small, non-enveloped, non-pathogenic dependoparvovirus which was discovered in 1965 as a co-infecting contaminant in infections of the common cold virus, Adenovirus (Atchison et al., 1965). The AAV genome comprises of 4.7kb single strand DNA encoding for Rep protein (for replication and packaging) and Cap protein (for capsid structure), flanked by two hairpin structure ITRs (inverted terminal repeat) (Vance et al., 2015). To perform its infection, AAV requires a helper virus, for example, adenovirus or herpesvirus. Recombinant AAV is created by removing the Rep and Cap gene and replacing the expression cassette containing the gene of interest. The size of a transgene to fit in AAV genome is around 4.7 kb. AAV vector has become a favorite vector to use in gene therapy thanks to its safety (no toxicity, no-known immunological response on human, no integration in host genome) and its efficient transduction efficiency *in vitro* and *in vivo*. There are >12 different serotypes that have been used in animal and human studies in a total of more than 100 natural variants of AAV. All of the rAAV vector was generated in research using the ITRs of AAV serotype 2's genome and then packaged in other AAV's Cap and Rep sequence provided *in trans*. Capsid sequence from AAV 1-9 has more than 80% homology except for AAV4 and AAV5 have the most divergent sequence. The difference is mostly located in the looped-out domains which are exposed to the surface of the capsid (Vance et al., 2015). Even a six amino acid difference between

AAV1 and AAV6 could dictate a different binding receptor of each AAV. The AAV7m8 serotype is a genetic variant of AAV2 containing 7 peptides (LGETTRP) disrupting its binding to heparan sulfate proteoglycan (HSPG) receptor (Chen, 2015; Dalkara and Byrne, 2013). It was isolated and characterized after an *in vivo*-directed capsid evolution by injecting a mixture of three libraries intravitreally into the mouse eyes and collecting the capsid libraries of AAV particles that could access to photoreceptors layer (Chen, 2015; Dalkara and Byrne, 2013). AAV8b was generated from *in vivo* directed evolution via inserting a random region in between the residues from amino acids 585 to 593 of the AAV8 capsid to target ON-bipolar cells (Cronin et al., 2014).

The tropism of each AAV serotype on each cell type/tissue is variable due to a complex molecular mechanism of AAV infection, such as interaction of AAV capsid with different receptors on cellular surface, endocytosis of AAV particles, the amount of AAV particles access to the nucleus. AAV2 requires heparin sulfate proteoglycan (HSPG), AAV9 needs N-terminal galactose, and AAV1, 4, 5, and 6 bind specific N- or O linked sialic acid moieties (Kern et al., 2003; Murlidharan et al., 2014). A genetic screening to detect the most significant enrichment of KIAA0319L gene during AAV2 infection suggested it encodes for a so called universal AAV receptor (AAVR) (Pillay et al., 2016). In addition, the expression of AAVR in cell lines specific AAVR knockout rescued the infection in multiple AAV serotypes (Pillay et al., 2016). However, the role of AAVR in every AAV serotypes infection pathway as well as whether or not AAVR is efficiently a universal receptor for all AAV serotypes need to further investigated (Summerford and Samulski, 2016). With the complexity of AAV infection and the diversity of AAV serotypes, one direct way to understand the expression of transgene using AAV is via screening the specific transduction efficiency of AAV serotypes on *in vitro* cellular models and/or animal model.

AAV mediated gene therapy: clinical trials

The first AAV mediated gene therapy product that was approved by the European Commission in 2012 was Glybera (alipogene tiparvovec). This AAV carries the human lipoprotein lipase gene which is delivered to treat lipoprotein lipase deficiency (Moran, 2012).

In the US, there have been recent great strides in gene therapy, with three gene therapy products approved by the US Food and Drug Administration in 2017. There are the first gene therapy products approved in the USA. The first is Kymriah (tisagenlecleucel), which is an ex vivo therapy for certain pediatric and young adult patients with a form of acute lymphoblastic leukemia (ALL). The second is Yescarta, a chimeric antigen receptor (CAR) T cell therapy designed for ex vivo treatment of certain types of non-Hodgkin lymphoma. And the third, is the first gene therapy in the USA designed to be injected directly into the diseased target tissue (the retina), Voretigene Neparvovec-rzyl. This is also the first gene therapy product approved to treat a blinding disease.

Luxterna is a recombinant AAV serotype 2 (AAV2) vector carrying a normal copy of the RPE65 gene, a gene which when mutated causes an autosomal recessive congenital form of severe blindness, Leber congenital amaurocis (LCA). The *RPE65* gene is normally expressed in RPE (Maguire et al., 2009, 2008; Russell et al., 2017). The success of Luxterna, which has reversed blindness safely and stably and bilaterally in the majority of eyes of the Phase 3 clinical trial subjects, paves for way for development of gene therapies for other monogenic progressive diseases affecting the retina, including choroideremia. Since cells in the retina do not divide after birth, the reagent can be delivered once without concern about the reagent being diluted out due to cell division.

There are several reasons why CHM is one of the lead contenders for additional success in developing a gene therapy product. First, almost all *CHM* mutations result is complete loss of functional REP1, suggesting that adding exogenous REP1 (through gene delivery) would rescue the disease phenotype. Second, the progression is slow so that time windows for the therapeutics is long. Third, the coding sequence of CHM is less than 1.5 kb allowing a comfortable fit in the AAV vector's cargo hold. Finally, the subretinal injection method is available to target directly and efficiently the cells in the retinal area like RPE or photoreceptors which were affected cell types in CHM (Peng et al., 2017).

The first gene augmentation clinical trial for choroideremia using AAV2 was initiated in the United Kingdom in 2011 (ClinicalTrials.gov Identifier: NCT01461213) (MacLaren et al., 2014). In this study, 6 male patients (age 35 to 63 years) were subretinally injected with 0.6 – 1E10 AAV2.REP1 vector genomes. The best corrected visual acuity in two patients at advanced stage of disease increased 21 and 11 letters compared to the untreated eye, and this improvement was maintained until at least 3.5 years after treatment. Three other patients did not show a significant change and one patient decreased in visual acuity. The microperimetry to measure retina sensitivity increased 2.3 dB on average. The safety profile is excellent with no adverse event for the eyes and no immune response (Edwards et al., 2016; MacLaren et al., 2014). With this initiation, additional sites initiated gene augmentation clinical trials for choroideremia using Nightstar as a sponsor. Recently, Nightstar announced initiation of a Phase 3 (registrational) trial for choroideremia (Nightstar Therapeutics, 2018b).

Meanwhile, in the U.S.A., Spark Therapeutics initiated a Phase 1/2 trial to evaluate the safety and preliminary efficacy of SPK-7001 on choroideremia patients (Spark Therapeutics, 2018). Given the high degree of safety of AAV2 after subretinal injection (as demonstrated in the RPE65 clinical trials and, subsequently, in the Nightstar

choroideremia trial), this was also chosen to be the gene delivery vector in Spark's multi-center CHM clinical trial. The latter trial was initiated in 2015 using a vector for which efficacy had been demonstrated *in vitro*, in iPSCs derived from individuals with choroideremia. So far, AAV2 has been relatively benign after subretinal injection in choroideremia, even though the region targeted is a region which is highly vulnerable to mechanical stress due to the fact that it is a single cell layer: the fovea. One outcome desired in these studies is that the intervention will allow the cells in the retina to persist for longer, and thus to provide vision for longer. Because the disease is slowly progressive, it may take several years to determine whether this reagent confers any benefit.

Meanwhile, additional studies aim to probe the utility of other recombinant AAV vectors that may have more desirable properties in terms of transduction of the RPE and photoreceptors.

CHAPTER 2 - MATERIALS AND METHODS

2.1. Human pluripotent stem cells generated from CHM probands

2.2. Retinal pigmented epithelium (RPE) differentiation

2.3. Transepithelial electrical resistance (TER)

2.4. Apical and basal secretion of VEGF and PEDF from RPEs

2.5. RNA isolation, cDNA synthesis and qRT-PCR analysis

2.6. Immunofluorescence

2.7. Recombinant Adeno-associated virus (rAAV) production

2.8. *In Vitro* Transduction efficiency mediated by different recombinant AAV serotypes

2.9. Transduction efficiency of different rAAV serotypes in Non-Human Primates (NHPs)

2.10. Prenylation assay

2.11. Phagocytosis Assays

2.12. Statistical Analysis

2.1. Human pluripotent stem cells generated from CHM probands

Primary peripheral blood mononuclear cells (PBMCs) were collected from four CHM probands carrying mutations in the CHM gene. The CHM gene mutations included 1) CHM-1 (JB-415, c.1327_1328delAT), 2) CHM-2 (JB-500, exon 2-4 deletion), 3) CHM-3 (JB-527, exon 2-4 deletion), and 4) CHM-4 (JB-588, Arg555STOP, AGA->TGA). Mutation validation was performed on patient derived iPSC gDNA using primers in Table 1. All human protocols were approved by the institutional review board (IRB) at the University of Pennsylvania and each donor provided signed informed consent (IRB 808828). PBMCs were expanded in SP34 media containing IL-3, IL-6, SCF, and FLT3 plus penicillin/streptomycin and glutamine. Reprogramming of expanded PBMCs were performed as previously described (Maguire et al., 2015). Cells showing iPSC morphology were collected and expanded in iPSC medium (iPSC.CM; DMEM/F12 (50:50; Corning) containing 1 x glutamine (Life Technologies), 1 x penicillin/streptomycin (Life Technologies), 15% Knockout serum replacement (KSR) (Life Technologies), 1 x NEAA (Life Technologies),, 0.1 mM β-mercaptoethanol (2-ME) (Life Technologies), and 5 ng/mL of bFGF (R&D Systems) on 0.1% gelatin-coated dishes with irradiated mouse embryonic fibroblast (iMEFs). Cell lines were expanded and characterized for morphology, pluripotency gene expression (cMYC, DNMT3B, Nanog, OCT3/4), surface markers expression (SSEA3-488; Biolegend 1:100, SSEA4-647, Biolegend 1:100), Sendai transgene clearance, and all g-banding analyses were performed by Cell Line Genetics, Inc. CHM iPSCs were cultured on 1:100 matrigel-coated dishes in StemFlex media (Invitrogen) to perform germ layer specific analysis; mesodermal cultures (days 0-2: RPMI media plus 1 μM Chir99021, 5 ng/mL BMP4, and 50 ng/mL VEGF), days 3-7: serum free media (SFM) containing (5 ng/mL BMP4, 50 ng/mL VEGF, and 20 ng/mL bFGF),

Endodermal (days 0-2: RPMI media plus 2 μM Chir99021, 50 ng/mL Activin-A), days 3-7: SFM media containing (0.25 ng/mL BMP4, 10 ng/mL VEGF, 5 ng/mL bFGF, and 50 ng/mL Activin-A), Ectodermal (days 0-7: DMEM/F12 media containing 2% B27, 1% N2, 100 nM LDN193189, 10 mM SB431542, and 2 μM XAV939). Cultures were collected after 7 days and analyzed for lineage-specific genes and compared to iPSC RNA. The primers for pluripotency and germ layer are provided in Table 2. The unaffected control iPSCs (JBWT2 (PBWT2), JBWT3 (PBWT3), JBWT4 (BMC)) were previously characterized and published (Mills et al., 2013; Sullivan et al., 2014).

2.2. Retinal pigmented epithelium (RPE) differentiation

iPSCs were cultured on 0.1% gelatin-coated plates containing iMEFs in 37^0C 5% O_2 5% CO_2 until initiation of RPE differentiation. Cell lines were placed in feeder independent growth conditions by passaging iPSC from iMEFs to matrigel-coated dishes using TrypLE (Life Technologies). Once placed on matrigel-coated dishes, cells were maintained in mTESR (Stem cell Technologies) medium until cells reached a confluence of 50-60%. At this confluence, cells were transferred to 37^0C 5% CO_2 incubator and RPE induction was initiated. The base media for days 0-14 was DMEM/F12 plus 2% B27 (ThermoFisher), 1% N2 (ThermoFisher), 1 x Penicillin/Streptomycin, and 1x Glutamax. On days 0-2 (48 h), cells were treated with Noggin (50 ng/mL), DKK1 (10 ng/mL), Nicotinamide (10 mM), and IGF-1 (10 ng/mL) feeding daily. On days 2-4 (48 h), cells were treated with Noggin (50 ng/mL), DKK1 (10 ng/mL), Nicotinamide (10 mM), IGF-1 (10 ng/mL), bFGF2 (5 ng/mL). On days 4-6 (48 h), Activin-A (100 ng/mL), IGF-1 (10 ng/mL), and DKK1 (10 ng/mL). On days 6-14 (9 days), Activin-A (100 ng/mL), SU5402 (10 μM), and VIP (1 nM). On day 15, media was switched to RPE media DMEM/ Ham's F12 (70:30),

2% B27, 1 x Glutamax, and 1 x Penicillin/Streptomycin. Cells were maintained in RPE media for 21 days. At day 35, cells were passaged using Accutase plus DNase1 using a two-step approach. Cells were initially treated for 20 min with Accutase + DNase1 to eliminate no-RPE cells, washed 2 x with PBS, and then treated with Accutase/DNase1 for 20 min. Cells were detached using p1000 and centrifuged at 1500 rpm for 5 min. Cells were suspended in X-Vivo 10 media containing ROCK inhibitor, Thiazovivin (2 μM). All subsequent expansion of RPE included addition of Thiazovivin (2 μM), which allows for extended passaging of iPSC-RPEs.

2.3. Transepithelial electrical resistance (TER)

iPSCs were grown on fibronectin coated (5 μg/mL: 1.66 μg/filter) transwell filters for 3-4 weeks post-passaging to establish a monolayer RPE culture. TER of iPSC-RPE cultures was measured using a volt-ohm meter following manufacturer's instructions (World Precision Instruments, Sarasota, FL). The TER was calculated by subtracting the background TER measurement from the fibronectin-coated transwell containing no cells from the TER recording of control or CHM iPSC-RPEs. Each iPSC-RPE cell line had a minimum of 9 transwells measured per individual and TER (Ω cm^2) was measured weekly after reaching confluence and displaying a cobblestone appearance.

2.4. Apical and basal secretion of VEGF and PEDF from RPEs

Control and CHM iPSC-RPE monolayers on transwells with a TER > 250 Ω cm^2 were fed with X-Vivo 10 media in both the apical (500 μl) and basal (1 mL) chambers. After 24 h, media was collected separately from each chamber (minimum of 9 per individual) and subjected to ELISA assay for secreted proteins; VEGF (R&D systems) and PEDF (R&D systems) in accordance with manufacturer's recommendations.

Basically, for VEGF ELISA, the VEGF primary antibodies were attached on the surface of the ELISA plate. VEGF protein standard at different dilutions as well as diluted supernatant from basal and apical chambers containing secreted VEGF from different lines of RPE cells were added into each well at triplicate. Human VEGF conjugated was added, incubated for 2 h and washed off. Substrate and stop solution was added in the final step. Color changes represents the amount of VEGF in the media. The optical density (OD) was measured using a microplate reader (Infinite M200Pro, Tecan) set to 450 nm and wavelength correction set to 540 nm. Standard curve was developed using the OD values of VEGF protein standard samples.

For PEDF ELISA, human Serpin F1 capture antibody were diluted and coated on ELISA plate (Costar) for overnight at room temperature (RT). Capture antibody was washed and blocking reagent containing 5% BSA was added for 1 hour at RT. 100 μL of various diluted standards and samples were added to each well in triplicate and incubate for 2 hours at RT. Next, samples and standards were washed away and human Serpin F1 detection antibody was added. Another wash step follows by addition of 100 μL Streptavidin-Horseradish Peroxidase (HRP). Then Streptavidine-HRP was washed away and substrate solution and stop solution were added accordingly. The optical density (OD) was measured using a microplate reader set to 450 nm and wavelength correction set to 540 nm. Standard curve development and results generation were similar to VEGF ELISA assay. Values were adjusted for differences in volume from apical and basal chambers.

2.5. RNA isolation, cDNA synthesis and qRT-PCR analysis

Total RNA purification was carried out on iPSC and RPEs as directed in PureLink™ RNA Micro Kit protocol (Invitrogen) including the optional on-column DNase step. RNA

was isolated from iPSC or RPEs and first strand synthesis was performed using TaqMan® Reverse Transcription Reagents. Protocol was followed as instructed by manufacturer, with each sample yielding a 20 μL reaction from 1 μg of RNA by using random hexamers as the primer type. cDNA was stored at -20 ^{0}C until needed for downstream analysis. For qRT-PCR, 10 ng of cDNA was mixed in a reaction containing 1 x Taqman Fast Universal PCR Master Mix (2x), 1 x TBP primer (VIC probes) and 1 x primers of specific target (FAM probes) and run in triplicate in a MicroAmp^R Fast Optical 96-well reaction plate (Applied Biosystems) using quantitation-comparative C_T ($\Delta\Delta C_T$) set-up of 7500 Fast Real-Time PCR system machine (Applied Biosystems). The specific primers for MITF, BEST1, Pmel17, TYR, N-cadherin, TBP were described in Table 2.

2.6. Immunofluorescence

RPEs plated on 8-well chambers were coated with 1:100 matrigel and placed in 37 ^{0}C incubator overnight. The next day media was removed and chamber slides with matrigel and their lids were placed at RT for 1 h. Cells were plated onto chambered slides by dissociating to single cells with Accutase (Invitrogen) using two-step approach described earlier in part 2.2., centrifuged, and resuspended pellet in X-Vivo media with ROCK inhibitor (2 μM Thiazovivin). Cells were maintained for a minimum of 3 weeks until a confluency of 100%, and hexagonal morphology had been reached and then prepared for fixation. Cells were fixed by adding 4% Paraformaldehyde (PFA) in PBS, and incubated at 4 ^{0}C for 30 min. Then they were washed twice with cold 1 x PBS and blocked with 5% horse serum, 2% goat serum, 3% BSA + 0.3% Triton X-100 in PBS at RT for 1 h. Slides were immunostained with N-Cadherin (ThermoFisher, mouse; 1:200), MITF (ThermoFisher, mouse; 1:100), ZO-1 (ThermoFisher; Rabbit; 1:300) in immunofluorescence buffer (5% horse serum, 2% Goat serum, 3% BSA + 0.1% Triton X-

100 in 1 x PBS) and incubated overnight at 4 ^{0}C. Next day, wells were washed 3 x with 1 x PBS, and stained with corresponding secondary antibody (Alexa Fluor^{R} 488 - Mouse 1:500; Alexa Fluor^{R} 555 - Rabbit, 1:500, ThermoFisher) and maintained in the dark for 2 h. Samples were subsequently washed and counterstained with Hoechst (DNA stain) for 10 min. Coverslips were mounted with ProLong Gold mounting medium (Invitrogen).

2.7. Recombinant Adeno-associated virus (rAAV) production

rAAV.CMV.CβA.eGFP serotypes panel. The enhanced green fluorescent protein (eGFP)-encoding cDNA was cloned under the control of the CMV enhancer, chicken beta-actin promoter plus a portion of the chicken beta-actin intron into the pAAV backbone plasmids. A panel of different rAAVs with 11 different capsid serotypes including AAV1, AAV2, AAV3, AAV4, AAV5, AAV6, AAV7, AAV7m8, AAV8, AAV8b, AAV9 was generated for use in *in vitro* and *in vivo* studies. Basically, AAV vector were generated by triple transfection into HEK293T cells and purified using CsCl at the Center for Advanced Retinal and Ocular Therapeutic (CAROT)'s AAV Vector Core. Silver staining as used for titration of each rAAV vector. Vectors were stored with 0.001% Pluronic F-68 at -80°C until just prior to use.

rAAV.CMV.CβA.hCHM. The human CHM cDNA was cloned under the control of the same CMV-CβA regulatory sequence used to drive eGFP (previously described) using AAV serotype 7m8 vector. Based on the titer of the rAAV vector and the cell number of treated samples, AAV7m8.hCHM was diluted to a dosage of 1E5 vector genome (vg)/cell for gene augmentation studies in iPSC-RPEs.

2.8. *In Vitro* Transduction efficiency mediated by different recombinant AAV serotypes

Wells were treated with 1E5 vg/cell of each rAAV serotypes. At designated time points after infection (24 h, 48 h, 72 h, 96 h), plates were imaged quantitatively for eGFP using a Typhoon 9400 Variable Mode Imager (GE Healthcare) with a 520BP40 emission filter and a 488-excitation filter, with the photomultiplier set at 570 V, the sensitivity set at normal and the focal plane to +3 mm. Images were analyzed for densitometry using ImageJ[31] and the Protein Array Analyzer plugin. Wells were normalized to negative controls lacking viral vectors. Samples were run in triplicate and run in three independent experiments.

2.9. Transduction efficiency of different rAAV serotypes in Non-Human Primates (NHPs)

The studies were performed in compliance with federal and institutional mandates. Adult normal-sighted cynomolgous macaques were housed and cared for at the animal facility at The Children's Hospital of Philadelphia (CHOP, Philadelphia, PA) under IACUC protocol #1061. Subretinal injections of AAV in NHPs were carried out under coaxial illumination through the operating microscope and after administering anesthesia as described (Ramachandran et al., 2017). NHPs were euthanized one month post-injection. Tissue was fixed in 4% paraformaldehyde in phosphate-buffered saline (PBS), cryoprotected in 30% sucrose overnight at 4 ^{0}C, and then embedded and cryosectioned (12 μm) when frozen in optimal cutting temperature media (Fisher Scientific Co., Pittsburg, PA, USA) on a Leica CM1850 cryostat (Leica Microsystems, Wetzlar, Germany) as previously published (Ramachandran et al., 2017). Sections were evaluated for direct

eGFP fluorescence after mounting sections with DAPI (4',6-diamidino-2-phenylindole) in Fluoromount-G (Southern Biotech, Birmingham, AL). To confirm the complete absence of eGFP in the sections that direct eGFP fluorescence was undetectable, immunofluorescent detection of eGFP using anti-eGFP primary antibodies (Molecular probes A11122; Life Technologies) at 1:200 dilution followed by Alexa Fluor^{R} 488 secondary antibodies at 1:200 dilution (Life Technologies) was carried out. After staining, slides were observed under a confocal laser-scanning microscope (Olympus Fluoview 1000).

2.10. Prenylation assay

RPE cultures were maintained on tissue culture dishes for a minimum of 2 months to establish a hexagonal morphology prior to analysis. iPSC-RPE cells were either untreated or transduced with AAV7m8.hCHM viral vectors at the multiplicity of infection (MOI) of 1E5 viral genome (vg)/cell. Cells were maintained in culture media for 3 weeks post-transduction, then washed with cold PBS and scraped to collect a cell pellet. Cell pellets were lysed using prenylation lysis buffer (25 mM HEPES pH 7.2, 40 mM NaCl, 2 mM DTE, 2 mM $MgCl_2$, 20 μM GDP, 10 μM $ZnCl_2$) with protease inhibitor cocktail. Cell lysates were cleared by centrifugation. The cytosolic fraction of the cell lysate was collected by ultracentrifugation at 100,000g at 4 ^{0}C for 1 h. Cytosolic fractions were used to perform *in vitro* prenylation activity. An *in vitro* prenylation assay was performed using [^{3}H]-geranylgeranyl pyrophosphate (GGPP) as a prenyl group donor, in presence of recombinant Rab geranylgeranyl transferase and Rab27 (custom order from Blue Sky Biotech, Worcester, MA) as described (Black et al., 2014; Vasireddy et al., 2013). Incorporation of radiolabeled prenyl groups into the Rab27 protein was measured by liquid scintillation analyzer (Tri-Carb^{R} 4810 TR, PerkinElmer). Prenylation reactions were

performed in iPSC- RPE from unaffected controls, CHM and AAV7m8.hCHM transduced cell lines.

2.11. Phagocytosis Assays

pHrodo™ *Escherichia coli* BioParticles® conjugate were purchased through Invitrogen, Carlsbad, CA. iPSCs grown on 8-well chambers were maintained until all monolayer cultures had a cobblestone appearance (approximately 3-4 weeks post-passaging). iPSC-RPEs were incubated with 300 μL of pHrodo™ BioParticles® conjugate (1 mg/mL) for 2h at 37 ^{0}C; thereafter, the cultures were washed 3 x with 1 x PBS to remove any residual pHrodo bioparticles (designated as 0h). RPE at 4, 8, and 24 h time points were fixed with 4% PFA for 15 min at room temperature, then washed 3 x with PBS. After washes, cultures were stained with Hoechst (1:2000, nuclear stain), washed and mounted using Prolong Gold mounting medium (Invitrogen) and imaged on an inverted microscope (Leica DI8; Leica instruments, Inc.). Mean fluorescent units were measured per cell for each time point in triplicate.

2.12. Statistical Analysis

Data from each experiment were collected from three unaffected individuals (controls) and 3 CHM donors. Statistical results are described as the mean value ± standard error of the mean (SEM). The statistical significance was determined using Student's T-test (between averaged control and CHM). Statistics were considered significant with a p-value <0.05. Asterisk corresponding to the p-value (*p <0.05, **p <0.01, ***p < 0.001).

For transduction efficiency comparison between 11 AAV serotypes in iPSC and iPSC-RPE, ANOVA with two factors (Excel's analysis toolpak) with replication to determine the relationship of cell lines and AAV serotypes on the gene expression effect (significance with p-value < 0.05, $F > F_{critical}$). To determine the significant effect of each AAV serotypes for each cell line, ANOVA with one factor was used, followed by the post-hoc test pair-wise comparison (XLSTAT add-ins) to determine the statistical differences of AAV-eGFP intensity across AAV serotypes and cell line type.

CHAPTER 3 – PRODUCTION OF CHM PATIENT DERIVED *IN VITRO* CELLULAR MODELS

Overview

To overcome the limitations and lack of availability of animal models of choroideremia, we utilized personalized *in vitro* cellular models and hypothesized that patient-derived cell lines exhibit pathophysiologic and biochemical characteristics of the CHM disease. In this chapter, we generated *in vitro* cellular models for choroideremia - induced pluripotent stem cells (iPSCs) from primary peripheral blood mononuclear cells (PBMCs) of different individuals with choroideremia and differentiate those iPSCs into an ocular cell type - Retinal Pigment Epithelium (iPSC-RPE) for further investigation.

Introduction

Choroideremia (CHM) is an X-linked disorder with an incidence of approximately 1:50,000 (MacDonald et al., 2009). CHM is a progressive retinal degenerative disease that is characterized by childhood-onset night blindness (nyctalopia), loss of peripheral vision, and progressive loss of neural retina, RPE and choroid in a peripheral-to-central fashion. The cone photoreceptor-enriched region of fine visual discrimination, the fovea, is spared until late in the disease, but ultimately, total blindness results from destruction of this area, typically after the fifth decade of life (Aleman et al., 2017; Sanchez-Alcudia et al., 2016). The disease-causing gene, *CHM*, encodes Rab Escort Protein-1 (REP1), a protein that enhances geranylgeranylation of ras-related GTPases, Rab proteins. The precise mechanisms by which lack of REP-1 in the retina leads to disease are unknown, however a lack of prenylation of specific Rab proteins (Rab27a, Rab6a, Rab38) leads to defects in trafficking of motile small vesicles which is implicated in the disease pathogenies of CHM (Bolasco et al., 2011; Köhnke et al., 2013). To date, more than 110 mutations have been found to result in CHM. In extra-ocular tissues, REP2 compensates for a lack of REP1 and so disease is limited to the retina (Köhnke et al., 2013; Larijani et al., 2003).

The primary retinal cell type leading to choroideremia is unknown, although evidence from engineered mice and zebrafish and cells from affected individuals indicate that the affected cells are likely involve RPE cells, photoreceptors or potential choroidal cells (Anand et al., 2003; Black et al., 2014; Cereso et al., 2014; Tolmachova et al., 2013, 2012; Vasireddy et al., 2013). Studies of CHM in mouse models are challenging in large part due to the fact that lack of Rep-1 is lethal *in utero* in this species. Use of conditional mutants has helped confirm that RPE and photoreceptor cells are likely primary cell types causing the disease although these animals are not faithful models of the disease and are also difficult to access. Further, the fact that the earliest symptoms of Choroideremia in

humans include nyctalopia and loss of peripheral visual fields together with the preservation of cone photoreceptor (foveal) function until late in the disease (Aleman et al., 2017) suggest that rod (but not cone) photoreceptors are affected early in the disease course. Because of the difficulties with *in vivo* models for Choroideremia and other retinal diseases, we and others have explored the approach of using pluripotent stem cell (iPSCs) models (Cereso et al., 2014; David A Parfitt et al., 2016; Vasireddy et al., 2013).

Retinal pigmented epithelial cells are a critical cell type for active investigations for retinal developmental models, cell transplantation, and are increasingly used for preclinical assessment of therapeutics (Bennett, 2017; Kamao et al., 2014). RPE are a thin layer of pigmented epithelium that are adjacent to the photoreceptors of the retina and the Bruch's membrane. The RPE monolayer provides numerous functions in the retina, such as protection against photo-oxidative stress, provision of nutrients (including secretion of growth factors and cytokines), maintenance of separation from the blood supply (in part due to integrity of apical and basal polarity) and removal of waste products (due in part to elimination of outer segments of photoreceptors through phagocytosis) (Gordiyenko et al., 2010; Sun et al., 2016).

In this study, we explored the utility of iPSC-RPE to study disease pathogenesis and a potential gene-based intervention in four different genetically distinct forms of CHM which together, represent the most common disease-causing mutations: splicing defects, deletions and premature stop signals. First step was to generate iPSCs from peripheral blood mononuclear cells (PBMCs) of four CHM patients. Cells from normal-sighted individuals were used as control. Pluripotency markers expression and differentiation capability into three germ layers were characterized in those iPSC lines. The next step was to differentiate these iPSC lines into Retinal Pigment Epithelium (RPE) using a series of retinal inducing factors (Noggin, DKK1, IGF1, and bFGF) and other factors

(Nicotinamide, Activin A, SU5402, and vasoactive intestinal peptide [VIP]) at appropriate time points (Buchholz et al., 2009; Uchholz et al., 2013). iPSC-RPEs were characterized by their morphology, physiological features (RPE markers expression, tight junction, polarization, and phagocytosis). iPSC-RPEs from CHM patients were confirmed to lack of REP1 expression and their pathophysiological features were characterized in the subsequent chapter.

Results

Development of human *in vitro* model of CHM using patient derived samples.

To investigate the impact of *CHM* mutations in a human biological system, we generated patient derived induced pluripotent stem cells from four CHM individuals. The role of REP1 has been studied in fibroblasts, blood, and RPEs (Cereso et al., 2014; Gordiyenko et al., 2010; Tolmachova et al., 2013). Previous *in vitro* studies have demonstrated that REP1 is involved in protein prenylation and trafficking of Rab proteins. Rab proteins are a family of small GTPases involved in vesicular trafficking. Post-translational geranylgeranylation of these Rab proteins is crucial for their membrane association and function. Transfer of the geranylgeranyl (prenyl) groups to the Rabs by a transferase requires an accessory component, REP1. Lack of REP1 in CHM affects the transfer of prenyl groups affecting the prenylation and trafficking of Rab proteins. Our preclinical proof of concept studies using AAV vectors delivering REP1 have shown the restoration of REP1 mediated Rab27a protein trafficking and prenylation in fibroblasts and iPSC derived from patients with *CHM* mutations (Black et al., 2014; Vasireddy et al., 2013). However, the role of *CHM* mutations in patient derived ocular cells such as retinal pigmented epithelium RPE, has not been extensively studied. To generate a model to study prenylation, phagocytosis, and Rab27a protein localization and trafficking

underlying ocular phenotypes in CHM, we established iPSCs using Sendai reprogramming methods (Maguire et al., 2015). Peripheral blood was obtained from four patients to generate iPSC representative of their CHM phenotypes. These cell lines were designated as CHM-1, CHM-2, CHM-3, CHM-4. Each cell line showed normal iPSC morphology and molecular genetic analysis confirmed that cells harbor mutations in the *CHM* gene (Figure 1A-B). Pluripotency surface (SSEA3/SSEA4) and gene expression marker show high expression in CHM and control iPSC (Figure 1C-D). The removal of transgene from Sendai virus vector was confirmed (Figure 1E). In addition, all cells studied were karyotypically normal over > 20 passages, and *in vitro* differentiation germ layer assay confirmed competency to generate mesoderm, endodermal and ectodermal lineage specific gene expression (Figure 1F-G). Upon confirmation of cellular defects in iPSC, we investigated the capacity of these patient cell derived cell lines to generate retinal pigmented epithelium *in vitro*.

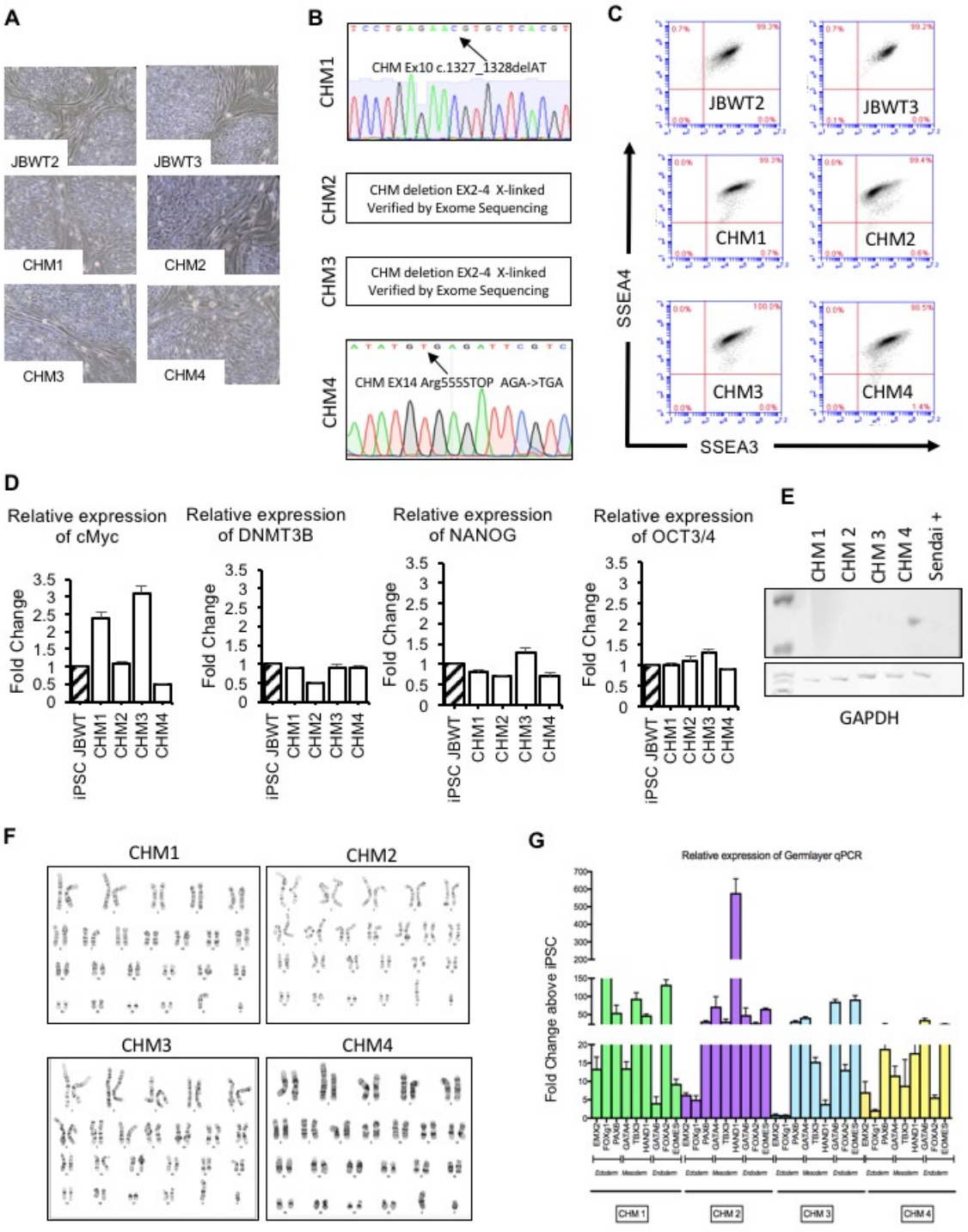

Figure 2. Analysis of iPSCs generated from patients with Choroideremia (CHM)

(A) Morphology of control and CHM-iPSC colonies. (B) Mutational analysis of affected donors: CHM1 (Ex10 c.1327_1328delAT), CHM2 and CHM3 have exon 2-4 deletions, and CHM4 (Ex14 Arg555STOP AGA->TGA). (C) Representative flow cytometry analysis plots of undifferentiated markers in control and CHM iPSCs: SSEA3/SSEA4. (D) Quantitative PCR (qRT-PCR) of relative gene expression of key pluripotency genes compared to control iPSC. (E) Transgene deficient iPSC lines shown by loss of Sendai genome. (F) Normal karyotyping of all four CHM iPSC lines. (G) qRT-PCR germ layer assay demonstrating efficient ectodermal (ECTO), mesodermal (MESO) and endodermal (ENDO) lineage-specific gene expression in CHM-iPS cell lines under induction conditions.

Generation of ocular specific cell type for modeling CHM *in vitro*.

Choroideremia patients exhibit progressive retinal degeneration leading to RPE atrophy and loss of peripheral vision throughout life. In order to develop a model amenable to studying the disease pathology of RPE development and maintenance, we investigated the capacity of CHM-iPSCs to generate monolayer cultures of RPEs. This was performed using a semi-confluent monolayer differentiation protocol which involves the addition of retinal inducing factors (DKK1, Noggin, Nicotinamide, Activin A, bFGF, VIP, SU5402 and IGF1) at specific time points to induce formation of RPE cultures as previously described (Buchholz et al., 2009; Uchholz et al., 2013). After 35-day post-induction, cells were passaged onto fresh matrigel-coated dishes and expanded to enrich RPE population. At passage 1, cells were plated onto matrigel-coated culture dishes and 8-well glass slides. After 3-4 weeks, cultures from three of the donors, CHM-1, CHM-2, and CHM-3, exhibited a similar "cobblestone" epithelial appearance on a phase contrast microscope, and protein expression of adherens junction marker (N-Cadherin and Zo-1), and RPE specific markers (OTX2 and MITF) (Figure 2A). Cells from the fourth donor, CHM-4, generated very few RPE cells after multiple tries, so they were not used for further iPSC-RPE experiments. Additional markers were evaluated in the CHM-1, CHM-2 and CHM-3-derived RPEs using qRT-PCR that showed high gene expression of key RPE markers; MITF, BEST1, Pmel17, TYR, and N-cadherin (Figure 2B). To verify cellular phenotype of CHM-derived RPE, we measured REP1 protein expression of control and CHM-RPEs and our analysis showed no expression in CHM-derived RPEs (Figure 2C).

To study polarized RPE cultures, we transferred control and CHM-RPEs to fibronectin coated transwell membranes and after 4 weeks of expansion all cultures exhibited morphologically identical hexagonal appearance. As establishment of tight junctions is a key element of the epithelial integrity of RPE, so we measured the

transepithelial electrical resistance (TER) across the monolayer of RPE grown on transwells. All control and CHM-RPEs demonstrated a transepithelial electrical resistance (TER; Ω cm^2) of greater than 250 Ω cm^2 (data not shown). Additionally, secretion of Vascular Endothelial Growth Factor (VEGF) and pigment epithelium derived factor (PEDF) was correctly localized to basal or apical aspects, respectively (Figure 2D). These data confirmed the establishment of an efficient and reproducible retinal cell type-specific *in vitro* model for studying Choroideremia. Taken together, our data indicates that RPE cultures developed from CHM and control iPSC lines exhibit the typical RPE phenotypes and show functional characteristics of RPE cells. CHM iPSC-RPE showed biochemical physiological defects due to REP1 lacking including a reduction in prenylation, a decrease in phagocytosis, an alteration of Rab27a protein trafficking and its localization. All of those features were confirmed and discussed in Chapter 5.

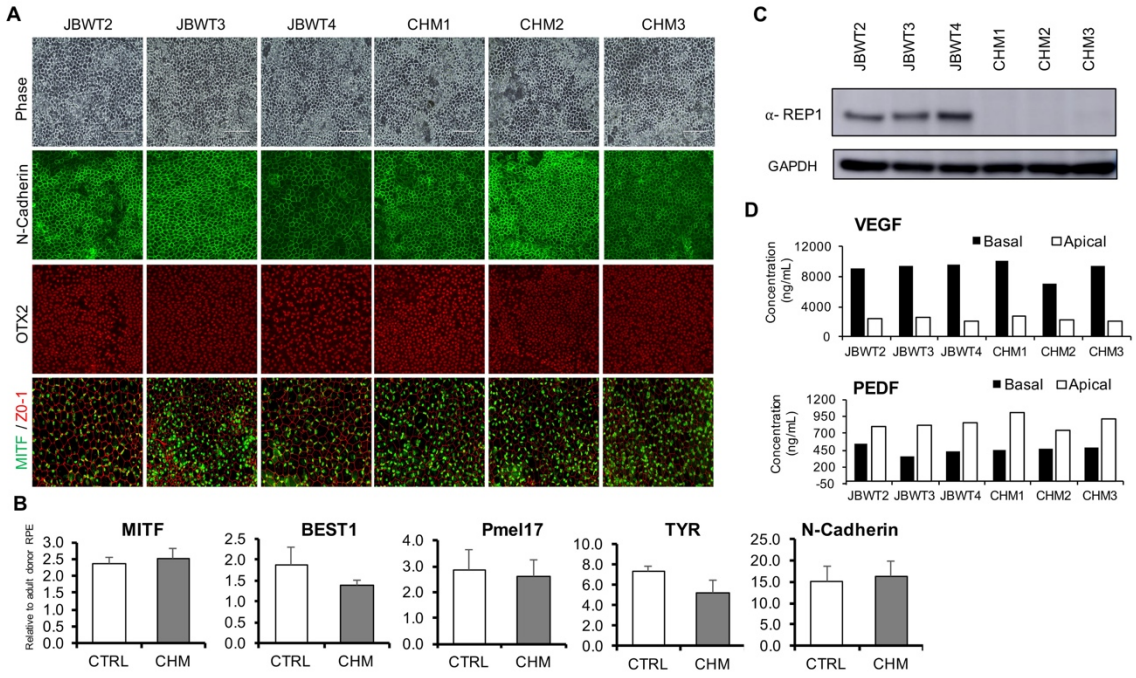

Figure 3. Generation and characterization of iPSC-RPE from control and Choroideremia (CHM) individuals.

(A) Representative Phase images of RPE morphology and protein expression of RPE markers, N-Cadherin, OTX2, and MITF/ZO-1 (green/red) in control (JBWT2, JBWT3, JBWT4) and choroideremia (CHM-1, CHM-2, CHM-3) iPSC-RPEs. (B) Quantitative RT-PCR shows gene expression of key RPE markers relative to donor RPE samples. (C) Western blot image shows lack of REP1 protein expression in all CHM-RPEs with corresponding GAPDH expression. (D) Polarized RPE protein secretion of VEGF and PEDF in control and CHM RPEs.

Summary

- **4 different CHM iPSC cell lines were generated and characterized their pluripotency.**
- **3 iPSC-RPE were successfully generated exhibiting RPE characteristics: RPE gene expression, RPE protein markers, polarization, and CHM cellular phenotypes of lacking REP1.**

CHAPTER 4 – *IN VITRO* AND *IN VIVO* TRANDUCTION EFFICIENCY OF AAV SEROTYPES

Overview

In order to find suitable AAV serotypes carrying CHM gene for our gene augmentation therapy on our *in vitro* cellular models and potentially for *in vivo* application in the future, we screened the transduction efficiency of AAV serotypes 1-9 panels (11 AAV serotypes) across various *in vitro* cellular models (iPSCs and RPE) and comparing the transduction efficiency of two best candidates (AAV5 and AAV7m8) on non-human primate model.

Introduction

With the discovery and evolution of AAV vectors for gene therapy, research has been focused on creating and choosing specific AAV serotypes to be able to deliver a transgene efficiently into the cell type/tissue of interest. Each of those serotypes has different tropism characteristics in different cell types or tissues. Endocytosis of AAV particles corresponding with the binding with different AAV receptors on the surface of the specific cell types. However, a direct screening of AAV serotypes on cell type of interest is critical. In this study, we perform a direct screening using 11 different AAV serotypes (AAV1, AAV2, AAV3, AAV4, AAV5, AAV6, AAV7, AAV7m8, AAV8, AAV8b and AAV9) carrying the identical reporter transgene cassette: an enhanced green-fluorescent protein (eGFP) gene driven by the cytomegalovirus immediate-early enhancer (eCMV) and chicken beta actin (CβA) promoter, which was transduced into two cellular models generated in Chapter 3: human iPSC, iPSC-derived RPE (Figure 4).

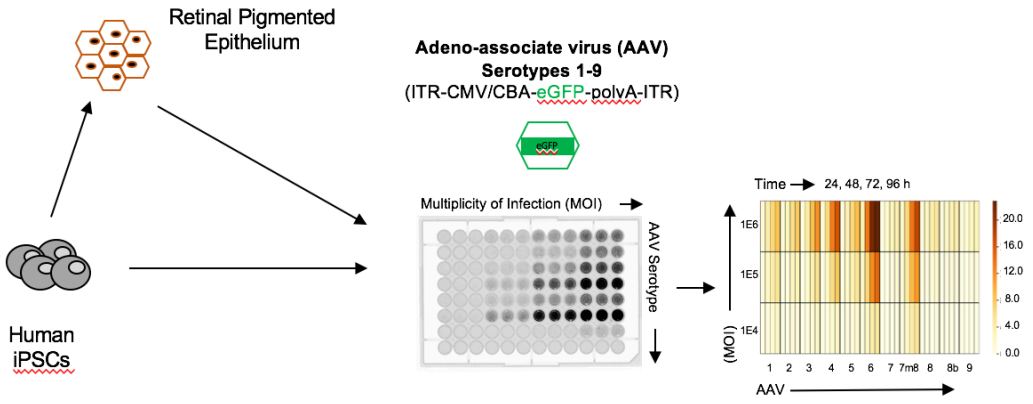

Figure 4. Transduction efficiency testing on iPSC and iPSC-derived RPE.

Human *in vitro* cellular models (iPSC and iPSC-derived RPE) were generated and cultured in their optimal condition. Before transduction efficiency testing, cells were collected and seeded at equal cell number in each well of two 96-well plates which were coated with matrigel previously. 11 AAV serotypes at different multiplicity of infection (MOI) were introduced to the cells in triplicate. GFP expression was measured by scanning the plate in Typhoon scanner followed by an analysis with protein array analyzer on imageJ. The transduction efficiency was normalized with background from untransduced wells and used as data to compare the critical effect of cell types and AAV serotypes on transgene expression.

Results

Transduction efficiency of AAV-eGFP panel in iPSCs and iPSC-derived RPEs.

Analysis of AAV tropism was performed on iPSCs derived from two individuals (JBWT2 and JBWT4), and cell lines were cultured in undifferentiated cell culture conditions to maintain a pluripotent state. Prior to transduction, cultures were observed for pluripotency cell morphological characteristics and surface markers expression (Figure 5A). iPSC cultures were transduced with 11 different serotypes at three different MOIs of 1E4, 1E5, and 1E6 vg/cell. The AAV-eGFP expression post-infection was recorded using live cell imaging using a Typhoon fluorescent plate reader at 24, 48, 72, and 96 h. The expression of GFP was observed to be dose and time dependent, and only at an MOI of 1E6 were all 11 rAAV expressed to measurable levels (Figure 5B-C). AAV-eGFP expression was first noticeable at approximately 48 h post-transduction and the level of expression stayed constant throughout the 96 h of experimentation. It is important to note that the iPSCs after 96 h are 100% confluent resulting in spontaneous differentiation;

therefore, the evaluation at later time points of the pluripotent state is no longer possible. There were significant differences across rAAV vectors used and the iPSC transduction efficiencies from highest to lowest were as follows at MOI: 1E6 vg/cells: AAV3, AAV7m8, AAV6, AAV2, AAV8, AAV1, AAV9, AAV8b, AAV4, AAV7, and AAV5 (Table 3). The group of higher transduction efficiency starts from AAV3, AAV7m8, AAV6 and AAV2 (≈ 3 to 5 folds higher than the low transduction efficiency group). The transduction with AAV7m8 was the only serotype to be expressed across all vector dosages (1E4, 1E5, and 1E6 vg/cell). The AAV-eGFP expression using AAV3 and AAV6 were the only other rAAVs to be expressed at more than one dosage (1E5 and 1E6 vg/cell). Identifying the appropriate AAV vector for gene delivery in pluripotent stem cells (PSCs) is important and expanding our repertoire of tools is essential. Previous work has investigated the use of AAV1, AAV2, AAV6, and AAV9 for transduction of PSC and demonstrated that AAV2 and AAV6 have the greatest tropism for pluripotent stem cells (Rapti et al., 2015). Our work supports these findings, and shows that AAV3 and AAV7m8 substantially increase transgene delivery and expression in additional serotypes for gene therapy of iPSCs. Moreover, the differentiation of pluripotent stem cells to ocular cells types are of profound significance as these areas are prime targets for gene augmentation strategies for therapeutic intervention.

RPE cells have been subject to a number of clinical interventions for the treatment of disorders associated with vision impairments such as retinitis pigmentosa (RP), Leber's congenital amaurosis (LCA), advanced neovascular age-related macular degeneration and choroidal neovascularization (Ghazi et al., 2016; Heier et al., 2017; MacLaren et al., 2014; Schnabolk et al., 2018). The differentiation of iPSCs to retinal pigmented epithelium (RPE) cells provide for structurally and functionally valuable tools for genetic and

therapeutic studies (Blenkinsop et al., 2015; Cereso et al., 2014; Vugler et al., 2008). Here, we expand the list of rAAV serotypes available for *in vitro* transduction of human iPSC-RPEs (Figure 5D). Similar to iPSCs, there were time, dosage and vector effects observed in iPSC-RPEs with and administration of 1E6 vg/cell. We identified 1E6 to be the only dosage with detectable AAV-eGFP expression among all rAAV serotypes (Figure 5E). AAV-eGFP fluorescence did not appear until 48 h similar to iPSCs; however, there was a time- dependent expression effect with maximal fluorescence intensity per cell being reached at 96 h post-transduction. RPE were able to be maintained on culture dishes for months post-transduction and eGFP expression was also maintained; moreover, the level of transgene expression remained consistent with expression measured at 96 h post-transduction (data not shown). In the majority of the rAAV serotypes administered, there was noticeable AAV-eGFP expression at the lowest MOI (1E4 vg/cell), but expression was increased by more than ~3-fold (1E5 vg/cell) and ~7-fold (1E6 vg/cell) at the higher MOIs across most rAAVs (Figure 5F). The increases in intensity or AAV-eGFP expression is not directly associated to the vector copy number increase (10 and 100 x, respectively), which could reflect a threshold for AAV endocytosis and processing of the capsids presented to RPE cells. A pattern of transduction efficiencies was observed in RPEs from highest to lowest were as follows at MOI: 1E6 vg/cells: AAV6, AAV7m8, AAV4, AAV3, AAV5, AAV1, AAV2, AAV8, AAV8b, AAV7, and AAV9 (Table 3). The higher transduction efficiency group includes AAV6, AAV7m8, AAV4, AAV3, AAV5, AAV1, AAV2 (~ 2 to 5 folds higher compare to other serotypes). *In vitro* screening has given a list of best candidates for our gene augmentation on iPSC-RPEs. Studying their performance *in vivo* is the next important step to decide which serotype is the best for CHM gene augmentation therapeutic intervention.

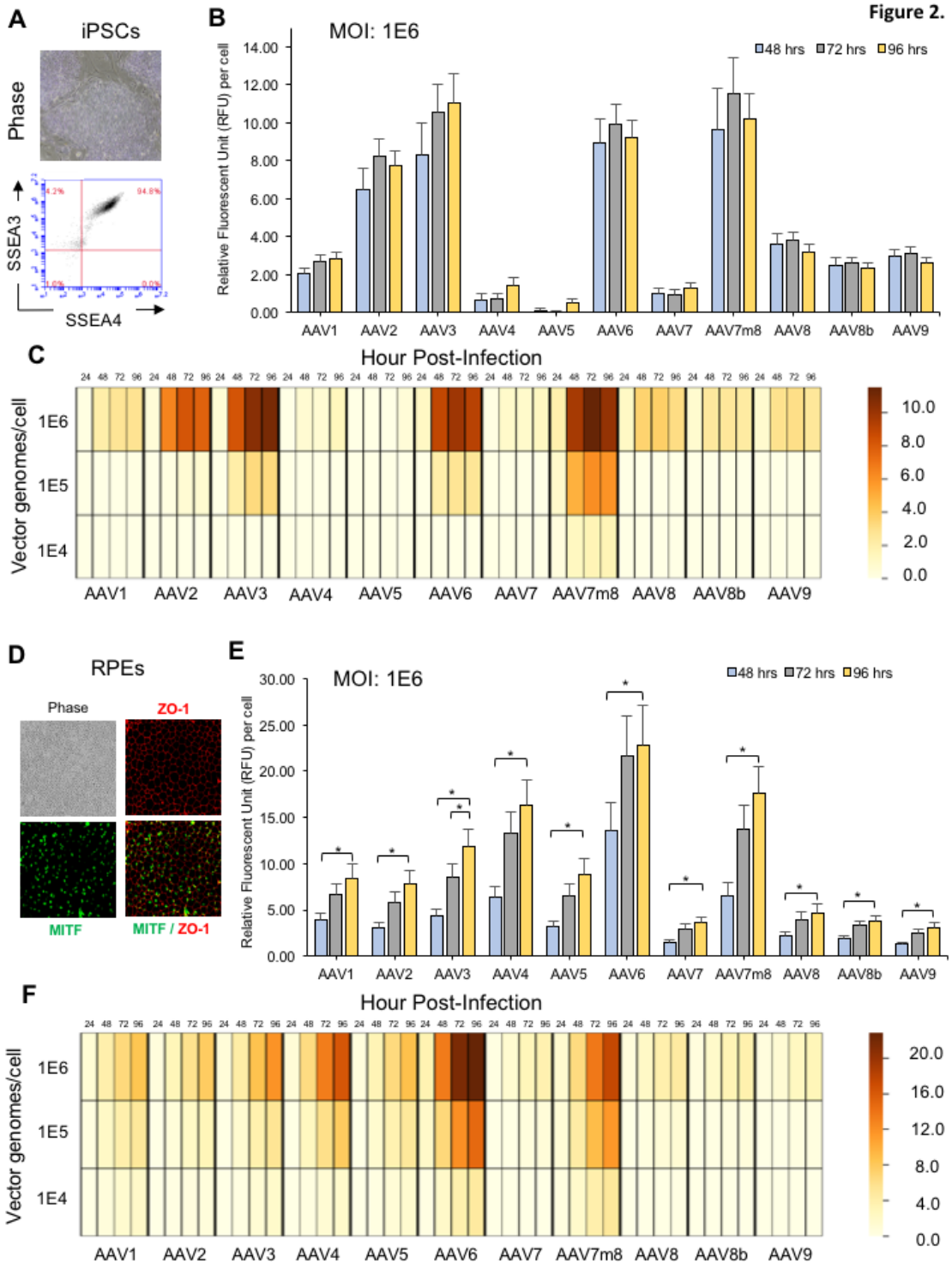

Figure 5. iPSC and iPSC-RPE tropism of 11 rAAV serotypes.

(A) Representative morphological and surface marker expression (SSEA3 and SSEA4) of pluripotent stem cells. (B) The onset of GFP expression in iPSCs at a dosage of 1E6 vg/cell for all rAAV at 48, 72, and 96 h post-transduction. (C) Heatmap showing relative AAV-GFP expression per cell across all rAAV, dosages, and time in iPSCs. The scale bar shows the intensity of AAV-eGFP expression presented as an arbitrary relative fluorescence unit (A.U) per cell. (D) Retinal pigmented epithelium (RPE) show "cobblestone" appearance with expression of ZO-1 (red) and MITF (green), and merged images showing uniform RPE monolayer. Images were captured at 20x magnification. (E) AAV-eGFP expression in RPEs at a dosage of 1E6 vg/cell for all rAAV at 48, 72, and 96 h post-transduction (F) Heatmap showing relative AAV-eGFP expression per cell across all rAAV, dosages, and time in RPE cells.

Non-human primate AAV5 and AAV7m8 transduction

We set out to determine which one of two rAAVs, AAV5 (previously noted to be the most efficient vector *in vitro* iPSC derived-RPEs studies by Cereso et al. (Cereso et al., 2014) and also ranking highly in our studies) and AAV7m8, created through evolutionary design (Dalkara and Byrne, 2013) and even more efficient than rAAV5 in our *in vitro* screen, might be most useful ultimately in human clinical trials (Figure 6A). To do this, we compared transduction efficiencies of AAV7m8 and AAV5 as a function of dose after subretinal injection in the non-human primate (NHP) retina. Since only primates (including humans) have a macula, a region of fine visual discrimination, NHPs seemed to be the most appropriate model. The goal was to identify the vector that was most efficient in targeting both rod photoreceptors and RPE cells as evidenced by expression of a CMV/CβA -driven reporter gene (eGFP) delivered by the AAV.

Transduction efficiencies of AAV5 vs AAV7m8.CMV.CβA.eGFP were compared in cynomolgous monkeys after subretinal injection of 1E10, 1E11, or 1E12 vector genomes (vg) and samples collected one month post-injection. As shown in Figure 6B, transduction of photoreceptors (occupying the outer nuclear, outer synaptic and outer segment layers), and RPE cells is far more efficient using AAV7m8 compared to AAV5. Further, rod photoreceptors are transduced efficiently with AAV7m8 but not AAV5. The latter mostly transduces cone photoreceptors (and only at doses >1E11 vg). AAV7m8 transduces rod (but not cone) photoreceptors at 1E10 vg, but both rods and cones at 1E11vg and higher. Thus, results from both the *in vitro* screen and from *in vivo* studies supported focusing further evaluations using AAV7m8.

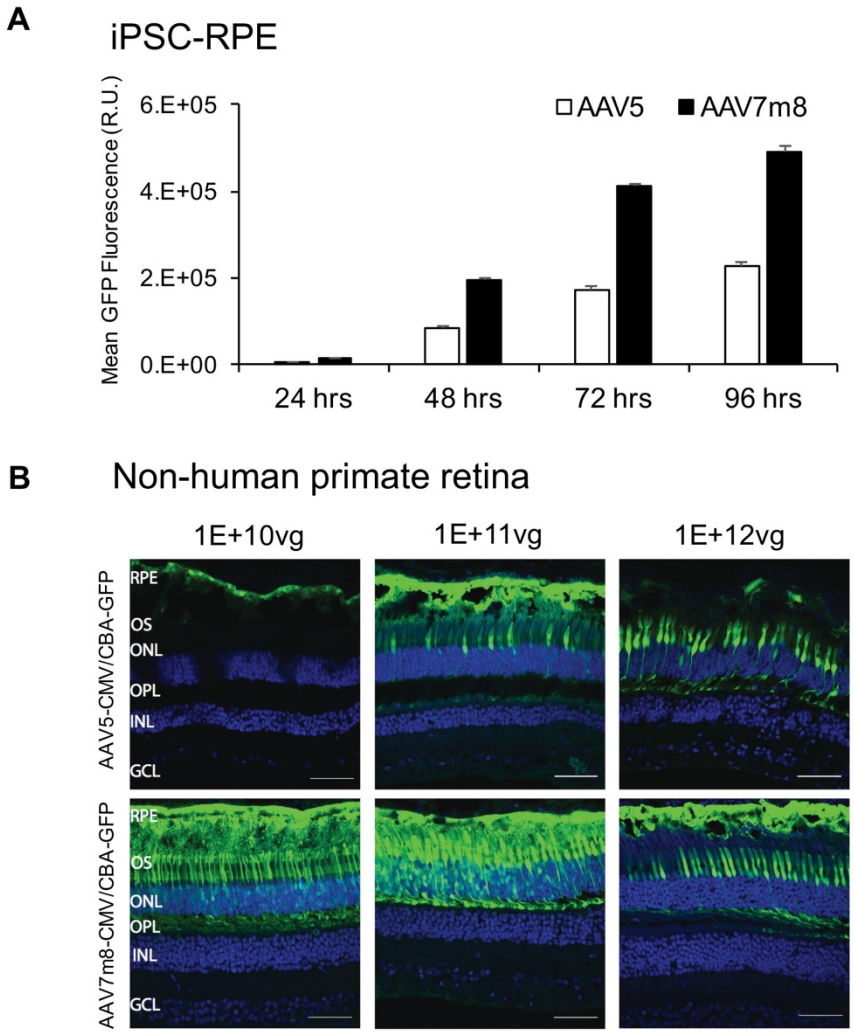

Figure 6. Transduction efficiency of recombinant AAV vectors A) in vitro and B) in vivo in the non-human primate (NHP) retina.

A) Transduction efficiency of iPSC-derived RPE cells generated from normal-sighted males (JBWT2 and JBWT4) using two rAAVs (AAV5 and AAV7m8) at an MOI of 1E5 vg/cell and all containing a chicken β actin (CBA) promoter with cytomegalovirus (CMV) enhancer driving enhanced green fluorescent protein (eGFP) cDNA. rAAVs delivered to cells were evaluated for intensity of eGFP at 4 different time points (24, 48, 72, and 96

hrs) post transduction. B) Comparative cellular transduction efficiencies in NHP retinas after subretinal delivery of AAV5 vs AAV7m8.CMV/CβA.eGFP over a dose range from 1E10 – 1E12 vector genomes (vg). Direct fluorescence of eGFP was evaluated histologically one month after injection. RPE, retinal pigmented epithelium; OS, outer segments; ONL, outer nuclear layer; OPL, outer plexiform layer; INL, inner nuclear layer; GCL, ganglion cell layer. Scale bars represent 40um.

Summary

- **For iPSC: We identified high *in vitro* transduction efficiency group (AAV3, AAV7m8, AAV6 and AAV2), and low *in vitro* transduction efficiency group (AAV8, AAV1, AAV9, AAV8b, AAV4, AAV7, and AAV5).**
- **For iPSC-RPEs: We identified high *in vitro* transduction efficiency group AAV6, AAV7m8, AAV4, AAV3, AAV5, AAV1, AAV2, and low *in vitro* transduction efficiency group AAV8, AAV8b, AAV7, and AAV9.**
- **AAV7m8 is the best candidate for both *in vitro* (iPSC, and RPE) and *in vivo* (Non-human primate, target Photoreceptors and RPE)**

CHAPTER 5 – GENE AUGMENTATION THERAPY USING AAV7m8.CMV.CβA.hCHM on iPSC-RPE

Overview

In this chapter, we studied the rescue effect of exogenous REP1 on iPSC-RPEs in term of prenylation, phagocytosis, protein trafficking.

Introduction

Current clinical studies for CHM focus on gene augmentation strategies using AAV2 and aim to prevent further degeneration and potentially also to enhance retinal function (Aleman et al., 2017; Edwards et al., 2016; MacLaren et al., 2014). Progression to the human clinical trial reported by Aleman et al was supported by the fact that AAV2-hCHM rescues prenylation and Rab27a protein trafficking in undifferentiated iPSC's derived from subjects with CHM mutations (Vasireddy et al., 2013). Recent clinical trials demonstrated the safety and efficacy of AAV2 mediated viral delivery (Edwards et al., 2016; MacLaren et al., 2014). In addition to delivering the transgene to RPE efficiently, high doses of AAV2 are required to target photoreceptors in non-human primates (Vandenberghe et al., 2011). In the present study, we further investigated the role of *CHM* mutations on cellular trafficking, phagocytosis, and RAB27a localization in patient-derived iPSCs differentiated into RPEs. We show that lack of REP1 leads to reduced and delayed phagocytosis, perinuclear accumulation of Rab27a, and inhibition of prenylation in three CHM patient-derived iPSC-RPEs. These defects are rescued by gene augmentation through the delivery with a vector that could be used in the future to deliver the transgene efficiently to the likely primary disease-causing cells, photoreceptors and RPE cells, in humans, AAV7m8-CHM.

Results

Adeno-associated viral delivery of hCHM cDNA rescues prenylation defect in iPSC-RPE.

The effect of mutations in the *CHM* gene on prenylation of Rab proteins in human iPSC-derived RPE was examined using an *in vitro* prenylation assay as previously

described (Köhnke et al., 2013; Vasireddy et al., 2013). This assay was developed to measure unprenylated Rabs in cell lysates, which had accumulated in RPE derived from CHM iPSC. To examine the AAV-mediated gene augmentation of REP1 in CHM-RPEs, we used CMV/CBA-hCHM vector packaged into AAV7m8 capsids. This was administered to the RPE cultures at 1E5 vg/cell (AAV7m8-hCHM). Transduced cultures were maintained for a minimum of 3 week prior to analysis and showed no change in morphology compared to untransduced CHM or control iPSC-RPEs. After ~3 weeks of treatment, RPE were collected and analyzed for REP1 protein content and the degree of prenylation in control, CHM, and AAV7m8-hCHM CHM-RPE. REP1 was present in the control samples (JBWT2, JBWT3, JBWT4) and absent in untreated CHM-RPE (CHM1, CHM2, CHM3); however, after CHM-RPE cultures were transduced with AAV7m8-hCHM, REP1 levels in CHM cells were comparable to those in controls (Figure 7A-B). To determine the level of unprenylated Rabs in RPE cultures, cell lysates were harvested and the cytosolic fractions were collected by ultracentrifugation and used for the *in* vitro prenylation assay. Using 3H-GGPP as the source of prenyl groups and cell lysate as the source of REP1, prenylation assays was carried out using incorporation of tritium-labeled GGPP as the read-out. As shown in Figure 7C, prenylation of RAB27 is significantly increased in AAV7m8-hCHM treated CHM-1, 2, 3 iPSC-RPE (~ 2-3 folds increase) compared to untreated control cells. The prenylation activity observed in AAV7m8.hCHM transduced iPSC-RPE is also found to be similar to the prenylation activity observed in unaffected controls (Figure 7D, ***$p < 0.001$). Thus, normal prenylation activity was present in three unaffected controls, and through gene augmentation using AAV7m8-hCHM we could rescue the prenylation defects observed in all three untreated CHM-RPE cell lines. To gain further insight into how loss of REP1 influences a key physiologic feature

of RPE, we investigated the capacity of these cells to digest pHRodo bioparticles during phagocytoisis.

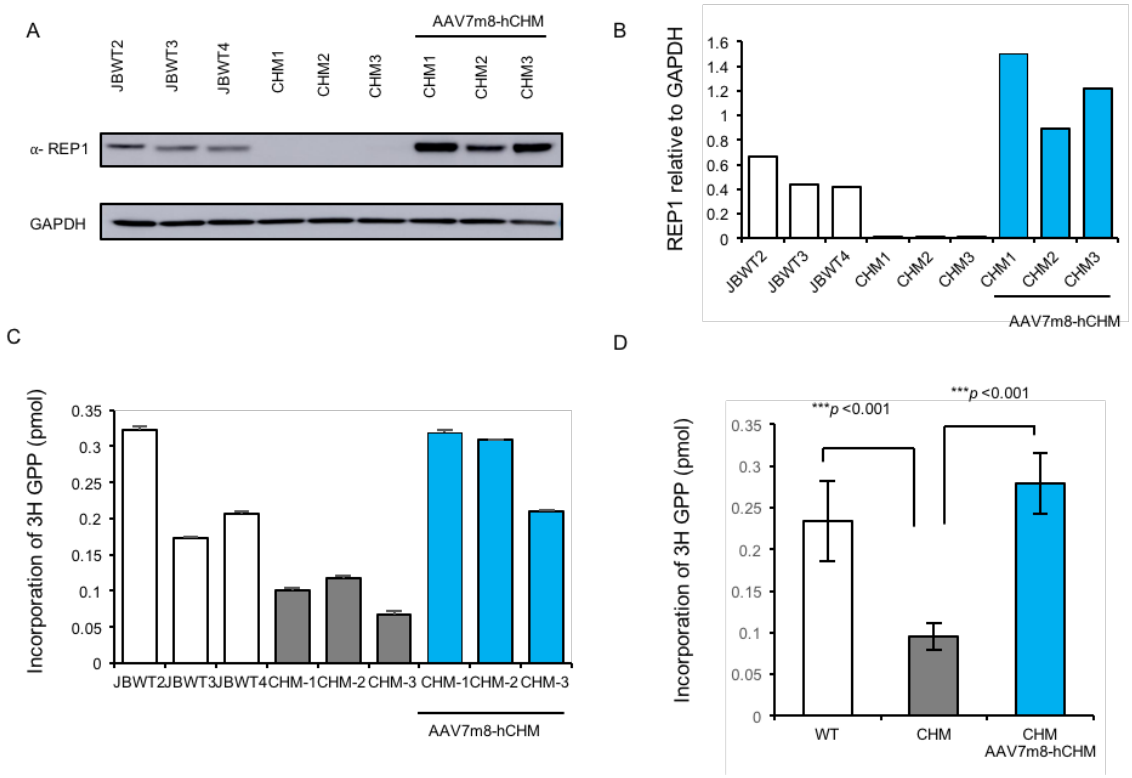

Figure 7. Effects of AAV7m8-REP1 gene augmentation on REP1 protein expression level and cellular prenylation.

(A) REP1 protein content in RPEs of three unaffected controls, three CHM individuals, and AAV7m8-REP1 (1E5 vg/cell) treated cultures. (B) Quantification of REP1 protein level compared to GAPDH. (C) Tritium prenylation assay shows lack of prenylation of Rab27a in CHM patient-derived RPEs (CHM1, CHM2, CHM3) and rescue after 1E5 vg/cell transduction of AAV7m8-hCHM viral vector. (D) Quantitative analysis of prenylation in control, CHM-REP1 deficient, and AAV7m8-hCHM treated RPEs.

Phagocytosis is impaired in CHM-derived RPEs.

Human and zebrafish models lacking REP1 show altered phagocyotosis. Further, shRNA silencing of normal REP1 expression in cultured cells has been reported to result in reduced phagocytosis activity (Gordiyenko et al., 2010; Koenekoop, 2007; Strunnikova et al., 2009). To investigate the phagocytosis and phagolysosomal activity of *CHM* patient-derived RPEs, we measured the ingestion of pHrodo *Escherichia coli* BioParticles (Invitrogen, Carlsbad, CA) through fluorescence of pHrhodo dye phagocytized bioparticles in our confluent monolayer cultures. The bioparticle fluorescence increases as the pH of the surroundings becomes acidic within the lysosome. After an initial 2h of exposure, the pHRodo particles were extensively washed from cultures and cells were incubated for an additional 4, 8, and 24h. The phagolysosomal activation was greatest after 4h of exposure to pHRodo particles and then declined over the 24 hours post exposure. The confluent iPSC-RPE monolayers showed a noticeable suppression of phagolysosome activation in *CHM* patient-derived RPE cultures when compared to the control (Figure 8A). To test whether gene augmentation of REP1 could rescue the phagolysosomal defect, we transduced *CHM* iPSC-RPEs with 1E5 vg/cell of AAV7m8-hCHM. All *CHM* patient samples treated with AAV7m8-hCHM had significant improvement in phagolysosomal activity compared to matched untreated *CHM* patient-derived RPE cultures at 4 and 8h after phRodo administration (Figure 8B, $^{**}p < 0.01$). These results demonstrate a suppression in RPE ingestion and phagolysosomal activation in *CHM*-derived RPEs, which can be rescued by AAV-mediated gene augmentation. The reduced phagocytosis has been suggested to involve the proper localization and action of prenylated Rab27a, which is necessary for vesicular transport which is disrupted by loss of REP1 in CHM.

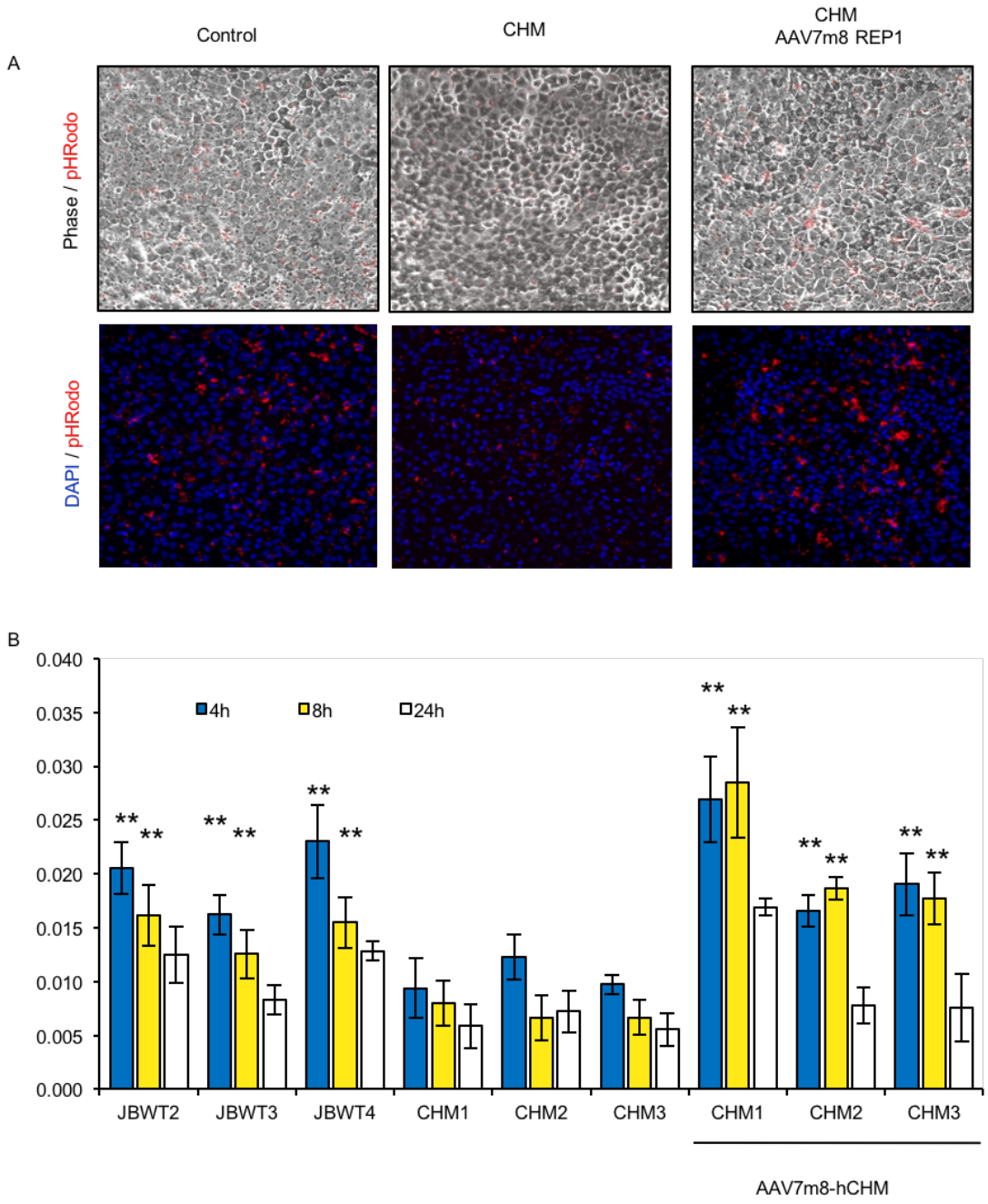

Figure 8. Effects of AAV7m8-REP1 gene augmentation on phagocytosis activation.

(A) Representative phase/pHRodo and Dapi/pHRodo images of control, CHM, and AAV7m8-treated CHM RPE show the ingestion of phRodo bioparticles in confluent RPE monolayers. (B) The relative fluorescent intensity was calculated for each culture after 4, 8, and 24h of exposure to pHRodo bioparticles

REP1 is required for the prenylation and cytosolic trafficking of Rab27a in human RPEs.

In view of our reported irregular distribution of Rab27a in CHM-IPSCs (Vasireddy et al., 2013), we directly assessed whether the distribution of Rab27a in pluripotency can be observed in multiple *CHM* patient-derived RPEs. The images presented in Figure 9A are representative of 4 separate cultures from each individual. We show that control RPEs (JBWT2, JBWT3, JBWT4) had detectable Rab27a that was dispersed throughout the cytosol of RPE cells. *CHM* patient-derived RPEs (CHM-1, CHM-2, CHM-3) had an average of 71% of cells with a dispersed cytosolic distribution, and the 29% cells had Rab27a that was found in the perinuclear region of the cell. The distribution across individual cells, perinuclear versus cytosolic, is shown in Figure 9B. We next determined whether overexpression of REP1 using AAV7m8-hCHM could result in recovery of the normal (pan-cellular) distribution of Rab27a. In the majority (81%) of the >150 cells analyzed per culture, Rab27a was dispersed throughout the cytoplasm after treatment with AAV7m8-hCHM similarly to that seen in WT control RPEs. Quantification of Rab27a biodistribution in untreated vs and AAV7m8-hCHM CHM RPEs shows that a significant proportion of REP1-positive cells have a cytosolic distribution compared to untreated REP1-negative CHM-RPEs (Figure 9B, $*p < 0.05$). Thus, this experiment directly demonstrates that prenylation of Rab27a by REP1 is required for vesicular trafficking and cytosolic distribution.

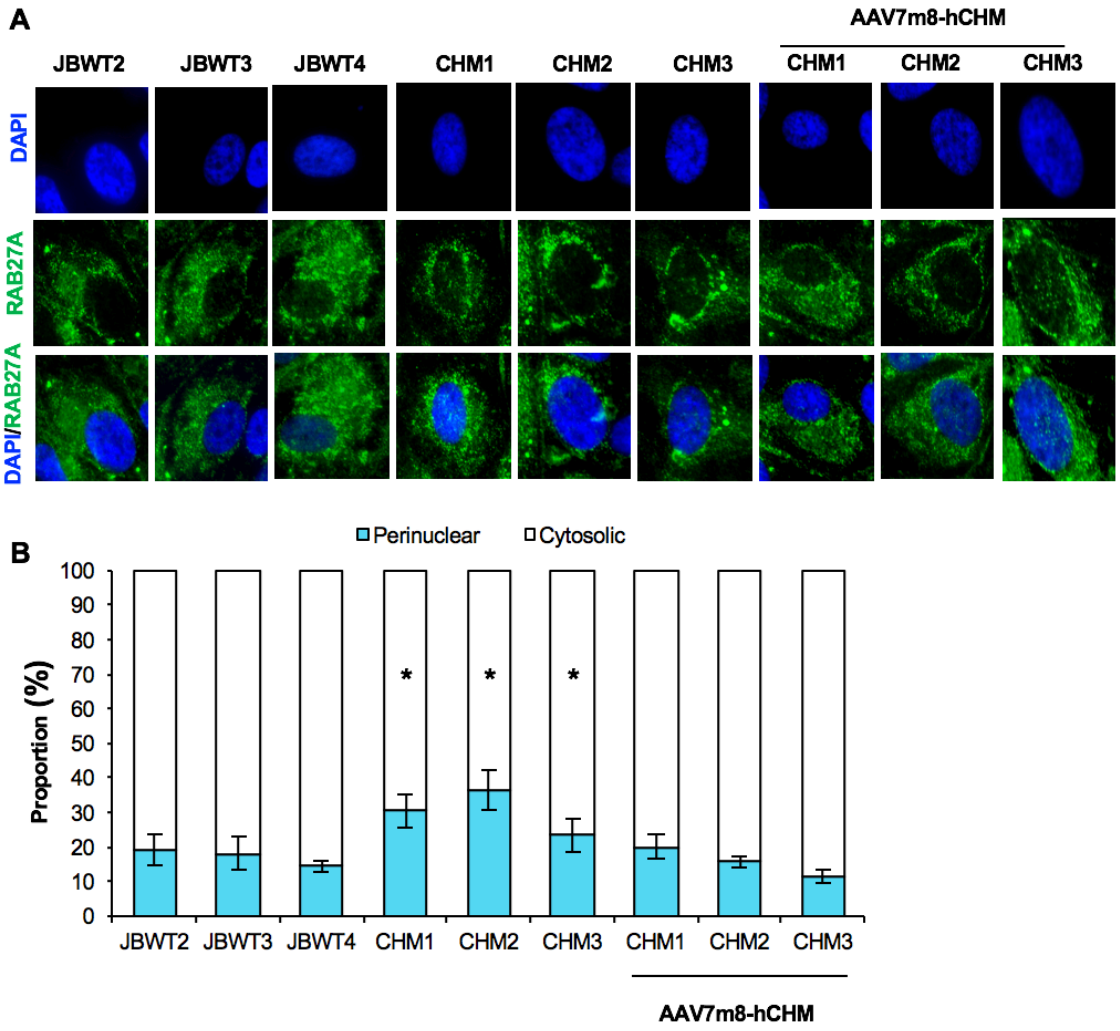

Figure 9. Mutations in CHM disrupt the localization of Rab27a and alter the onset of transgene expression mediated by AAV7m8 in wildtype (WT) vs mutant (CHM) human RPEs.

(A) Immunostaining for Rab27a protein localization (B) Rab27a localization is presented in a bar graph for perinuclear versus cytosolic distribution.

Internalization of AAV7m8 is reduced in CHM RPEs

A lack of REP1 in iPSC-RPE models alters the onset of transgene expression after transduction with AAV7m8-GFP. iPSC-RPE cells from normal-sighted individuals (JBWT2 and JBWT3) and from individuals with CHM (CHM-1 and CHM-2) were transduced with AAV7m8.CMV/CβA.eGFP at an MOI of 1E5vg/cell and onset and levels of GFP protein were imaged as a function of time after transduction. As shown in Figure 10, GFP was detectable by the 24hr timepoint in all RPE cell lines, with WT controls having significantly more GFP expression up until 48h post-transduction compared to CHM-RPEs (***p <0.001). Interestingly the GFP expression was normalized between the two groups by 72h. This data indicates that there is significant impairment in CHM-RPEs in one or more of the steps required in order to obtain AAV-mediated transgene expression compared to control RPEs.

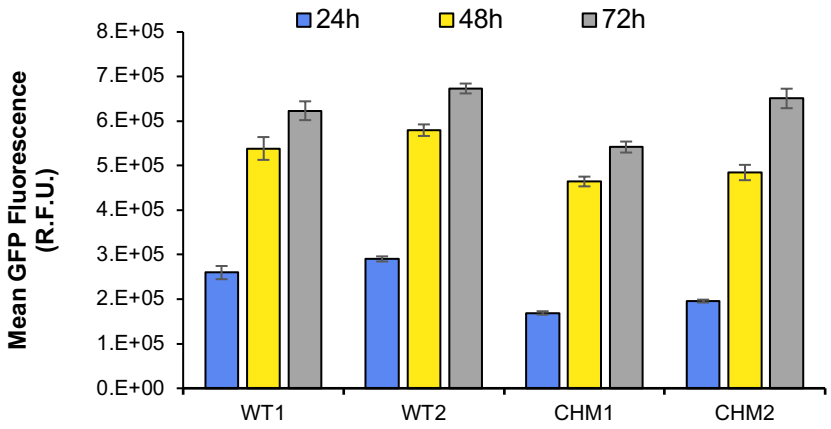

Figure 10. Mutations in CHM alter the onset of transgene expression mediated by AAV7m8 in wildtype (WT) vs mutant (CHM) human RPEs.

Transduction efficiency of control-RPE (JBWT2 and JBWT4) and CHM-RPEs (CHM-1 and CHM-2) using rAAV-7m8-CMV/CBA.eGFP at an MOI of 1E5 vg/cell over a period of 72h.

Summary

AAV7m8.CMV.CβA.hCHM to choroideremia iPSC-RPEs restored normal REP1 protein expression, prenylation, phagocytosis, and Rab27a protein trafficking.

CHAPTER 6 – DISCUSSIONS AND FUTURE DIRECTIONS

Choroideremia is an X-linked recessive monogenic disease caused by loss of function of REP1 protein that results in progressive degeneration of RPE, photoreceptors and choroid. The purpose of this study was to examine potential pathology induced by REP1 deficiency in retinal pigment epithelium cells of CHM patients and to investigate the potential for rescue using a gene augmentation strategy. There are three stages in our research: 1) generating iPSC and iPSC derived RPE as disease cellular models (Chapter 3), 2) screening and choosing the best AAV serotypes for gene augmentation study (Chapter 4), 3) studying rescue effect of AAV7m8.hCHM on the ocular affected cell type of CHM (Chapter 5).

With the limitation of CHM animal models as well as a need to find a suitable model to study molecular mechanism of the disease, we generated patient derived CHM cell lines which would be a useful resource to study the pathophysiology of CHM. In this study, we reprogrammed four different cell lines for peripheral blood mononuclear cells (PBMC) from four individuals carrying mutations in the *CHM* gene (nonsense, deletions, splicing defect). Although the cellular disease phenotype, including a decrease in prenylation and the mislocalization of Rab27a protein, were demonstrated in these patient derived iPSC models (Vasireddy et al., 2013), the specific retinal cell type affected by CHM need to be identified to reveal the precise role of REP1 in disease development.

Three iPSC derived RPE cell lines were generated from three unrelated patients with mutations in *CHM* gene. CHM-1 iPSC-RPE has a deletion of two nucleotides, Adenine and Thymine, at the location of 1327-1328 in the *CHM* cDNA sequence causing nonsense mutation and a truncated REP1 protein (p. I460X). This mutation affects the

structure, stability and function of REP1 protein (Strunnikova et al., 2009). CHM-2 and CHM-3 iPSC-RPEs have a deletion of exons 2-4 resulting in no function of the protein REP1 as well. A genotype-phenotype analysis of those nonsense and deletion mutations showed no clear correlation in term of visual acuity, visual field, onset of symptoms (Freund et al., 2016). In fact, lack of functional REP1 protein is the common phenotype in all three patient cell lines and it was confirmed by western blot (Figure 7).

Testing the tropism of a panel of 11 AAV-eGFP serotypes 1-9, 7m8, 8b revealed different patterns and fluorescent intensities of transgene expression in our *in vitro* cellular models including iPSC and RPE. This indicated that not only the rAAV serotype or the dosage of viral particles but also the cell type affects the level of transgene expression. Chapter 4 showed the transduction efficiencies listed from high to low on iPSC and RPE. Knowledge of the transduction efficiencies and cell tropisms is essential for selecting the appropriate vector to provide the required levels of transgene expression for a given application. In fact, having the highest level of expression will not always provide optimal results as the biology associated with transgene element needs to be considered. The endogenous level and transgene function: transcription factor, structural protein, chaperone, enzymes all need to be evaluated during gene augmentation testing. Our main focus is to select the optimal AAV serotype for *in vitro* gene augmentation therapy on iPSC-RPE and use that information to select the vector with the greatest potential for efficacy *in vivo*. AAV7m8 performs the best due to its optimal transduction efficiency *in vitro* even at low MOI (decrease dosage) as well as its infection capacity *in vivo* with respect to RPE and photoreceptors of the non-human primate model (therapeutic efficacy). The amount of REP1 protein produced after transduction with AAV7m8 is 1.5 fold higher than endogenous REP1 in the wild type iPSC-RPE. Previous studies in mice showed that overexpression of REP1 by subretinal injection of 1E8 to 1E9 genome copies

of AAV2.CMV.CBA-REP1 did not cause toxicity in mice as assessed by retinal function (Berndt and Sebti, 2011). Flow cytometry analysis of transduced CHM iPSC-RPE with AAV7m8.hCHM revealed a heterogeneity of level of REP1 expression in individual cells.

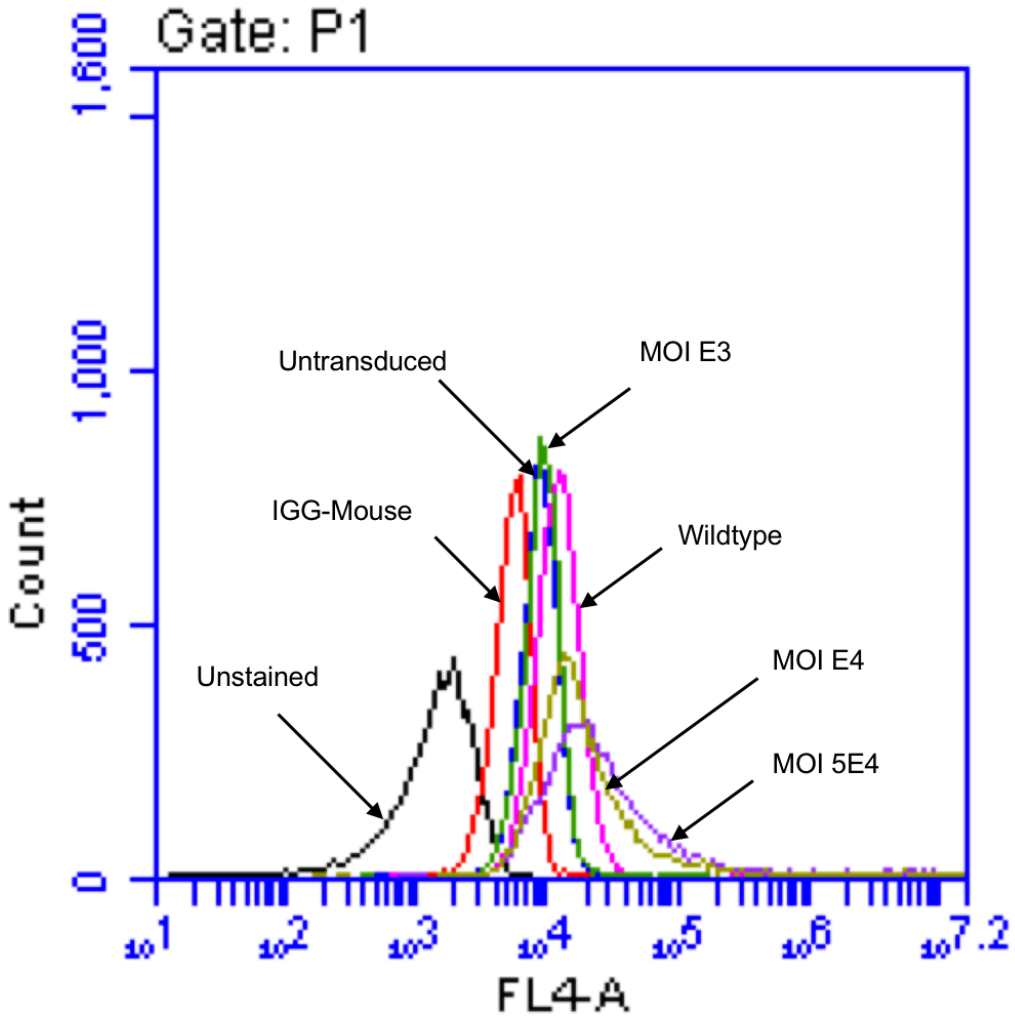

Figure 11. Flow cytometry analysis of REP1 in wildtype, untreated, transduced population of iPSC-RPE.

IPSC-derived RPEs have become a valuable resource for studying patient-specific retinal pathophysiology; therefore, we generated pluripotent stem cells from CHM-mutant somatic cells and then differentiated them into RPE. In previous studies, we used undifferentiated mutant CHM cells for study (fibroblasts and induced pluripotent stem cells) and showed that those cells are defective in prenylation of Rab proteins (Anand et al., 2003; Black et al., 2014; Vasireddy et al., 2013). Here, by differentiating patient-derived iPS cells into a retinal cell type, we are able to probe for other CHM-associated cellular phenotypes, metabolic processes (prenylation defects), and signs of cell biologic malfunction (suppressed phagolysosomal activation, alterations in protein trafficking).

Efficient prenylation of Rabs (mediated by REP1) is particularly important in preventing vesicular trafficking defects in cells responsible for protecting against oxidative stress and for serving as mediators of both nutrition and waste management , roles known to be played by the RPE (Strunnikova et al., 2012, 2009; Zhang et al., 2015b). Cereso et al. previously showed that iPSC-RPE cells display morphologic features typical of RPE cells (including a polarized epithelium with microvilli and desmosomes on the apical size, melanosomes distributed throughout the cytosol and a nucleus on the basal side), and that these cells express genes known to be expressed specifically in RPE cells (such as MERTK, RPE65, TYR) (Cereso et al., 2014). Further, these cells display many activities known to take place by RPE cells, such as apicobasal fluid internalization of particles presented to the surface of the cells. Cereso et al. also showed that CHM mutant iPSC-RPE cells manifest a prenylation defect and that this defect can be addressed through AAV5-mediated delivery of a wildtype *hCHM* cDNA (Cereso et al., 2014). Here, we use iPSC-RPE cells to further probe RPE cells with CHM mutations for defects in cellular and physiologic functions and for the ability to correct these defects using AAV-mediated gene transfer.

The approach to track biochemical effect of lacking REP1 in the patient cell line in Cereso et al.'s method and our study is *in vitro* prenylation assay. In our 3H-GGPP radio-labeling method, we measure the under-prenylation of exogenous Rab27a in the reaction with the presence or absence of endogenous REP1 protein. Cereso et al used BGPP (Biotin labeled BGPP) as a lipid donor to track the amount of endogenous Rab27a in the cytosolic fraction via estimating biotinylated Rab27a using Streptavidine horseradish perosidase after *in vitro* prenylation reaction. Overall, this *in vitro* prenylation assay can only can reveal the enzymatic activities of geranylgeranyl transferase with the support of REP1 in the Rab27a substrate. A more interactive method to functionally study the role of REP1 is an *in vivo* prenylation assay, through which we could determine the localization of unprenylated Rab in the cytosolic fraction and prenylated Rabs in the membrane fraction of the cells (Berndt and Sebti, 2011). In this method, it is necessary to optimize the method of subcellular fractionation to clearly separate cytosolic and membrane proteins and estimate the amount of Rabs protein in each component.

We found that CHM-iPSC-RPEs had reduced phagocytic activity as measured by numbers of particles ingested over time. They also showed suppressed phagolysosomal activation compared to control cells or isogenically matched CHM iPSC-RPEs that were treated with AAV7m8-CHM. The reduced activity was found in each of the genetically distinct iPSC-RPE cell lines that was evaluated. This reduced phagocytic activity likely contributes to impaired function of both RPE cells and rod photoreceptors. The reduced phagocytic activity is likely a downstream effect of prenylation defects associated with loss of REP1. In support of this, there was a reduced ability to prenylate the substrate Rab27a protein in each one of the CHM iPSC-RPE cell lines. As predicted, there was no clearcut difference in prenylation activity in each of the mutant cell lines because each of the genetically distinct mutations (splice site, deletion, premature stop) likely resulted in a

complete lack of REP-1 protein, a protein necessary for prenylation. The fact that phagolysosomal activity in CHM iPSC-RPEs was present (although reduced), could explain why there is fairly good retinal function early in life. Light exposure and resultant oxidative stress together with accumulation of metabolic and protein trafficking dysfunctions caused by reduced phagocytosis and ability to process waste products efficiently likely lead to progressive RPE and photoreceptor malfunction and degeneration over time.

We also found evidence of impaired intracellular protein trafficking and vesicular transport in the CHM-iPSC RPEs, likely also resulting from prenylation defects. This evidence includes the disproportionate pericellular accumulation of Rab27a in CHM-iPSC RPE, which was more than double that of control and AAV-treated iPSC-RPEs. Additional data supporting a defective trafficking was a delay in onset of rAAV-mediated GFP expression in CHM-RPEs compared to controls. This could be due to inefficiency in any one of a host of steps starting with contact of the AAV with the cell surface receptor and including endocytosis. Previous studies have shown that Rab27a is an important mediator of endocytosis in multiple systems (Ejlerskov et al., 2012; Yamaoka et al., 2016).

Impairment could also result in defective trafficking of the AAV to appropriate cellular compartments and ultimately through the nucleus pore, and then finally defective transformation of the single-stranded AAV DNA into the transcriptionally competent double-stranded DNA within the nucleus (Ejlerskov et al., 2012; Yamaoka et al., 2016).
The good news is that the defects we observed in CHM iPSC-RPE cells can be reversed through efficient delivery of the wildtype hCHM cDNA. Using both iPSC-RPE cells and primate retina to identify an AAV serotype that most efficiently transduces the cell types thought to result in CHM disease, AAV7m8, we show that prenylation, phagocytic activity,

and protein trafficking defects could be reversed. This set of data provides further support for the promise of gene augmentation therapy for choroideremia.

Localization of Rab27a is evaluated by immunocytochemistry. Another approach to determine the position of the protein by using flow cytometry. In this method, it is very critical to mask the boundary of cell compartment and the sensitivity of antibodies. Trafficking of other Rab proteins needs further investigation. The studies of RPE pigmentation and melanosome trafficking to the apical side after introducing exogenous REP1 is one more interesting aspect for future study. In our studies, the iPSC-RPE from CHM lines showed more pigmentation compared to control. Whether or not this accumulation of melanosome pigment is due to impaired trafficking is of future interest.

Table 1. Details on mutation analysis of four CHM patient cell lines.

CHM cell line	Patient annotation	Mutation	Primers	Mutation confirmation via Exome sequencing
CHM1	JB 415	CHM ex10 c.1327-1328delAT	CHM_Ex10_F: TCTTAGAGCTGTGAAGGGGG CHM_Ex10_R: CTCCACCCATTAGCAAGCGA	N/A
CHM2	JB 500	Exon 2-4 deletions	N/A	Yes
CHM3	JB 527	Exon 2-4 deletions	N/A	Yes
CHM4	JB 588	CHM Ex14 Arg555Stop (AGA → TAG)	CHM-Ex14-F: AATAGAAGTCCAAAGGAGCATGA CHM_Ex14_R: AGGGCAAATTACAGAAATGGTAC	N/A

Table 2. Primers for iPSC, RPE characterization.

Housekeeping	**GENE**	**Primer Orientation**	Cat number
	TBP	Predesigned Set	Applied Biosystems: Cat no. 4325803
RPE Characterization	**GENE**	**Primer Orientation**	**IDT ID**
	Nanog	Predesigned Set	hs04260366_g1
	DMNT3B	Predesigned Set	hs00171876_ml
	POU5F1 (OCT3/4)	Predesigned Set	hs00999634_gh
	cMYC	Predesigned Set	hs001153408_ml
RPE Characterization	**GENE**	**Primer Orientation**	**Sequence**
	MITF	Forward	CCTGTATGCAGATGGATGATGT
		Reverse	CCGAGACAGGCAACGTATTT
		Probe	TCTTGGGCTTGATGGATCCTGCTT

	TYR	Forward	CTTACTCAGCCCAGCATCAT
		Reverse	GGGCGTTCCATTGCATAAAG
		Probe	AGCCGATTGGAGGAGTACAACAGC
	N-Cadherin	Forward	GACAATGCCCCTCAAGTGTT
		Reverse	CCATTAAGCCGAGTGATGGT
		Probe	TCTGGAGTTTCGCAAGTCTCTGCC
	PEDF	Forward	CCCAAGCTGAAGCTGAGTTAT
		Reverse	GTTTGCCTGTGATCTTGCTAAAG
		Probe	CAGGGACTTGGTGACTTCGCCTTC
	BEST1	Forward	CTCAGTGTGGACACCTGTATG
		Reverse	CCCAACTAGACAAGTCAGGAAG
		Probe	ATACACAGGTGGTGACTGTGGCG
	PMEL17	Forward	GTTGATGGCTGTGGTCCTTG
		Reverse	CAGTGACTGCTGCTATGTGG
		Probe	AGGCGCAGACTTATGAAGCAAGAC T
Germ Layer Assay	**GENE**	**Primer Orientation**	**Sequence**
Ectoderm	EMX2	Forward	GCT TCT AAG GCT GGA ACA CG
		Reverse	CCA GCT TCT GCC TTT TGA AC
		Probe	TC AGC CTC AC GGA AAC TCA GGT AA
	FOXG1	Forward	GCC ACA ATC TGT CCC TCA ACA
		Reverse	CGG GTC CAG CAT CCA GTA G
		Probe	CAACAAGTGCTTCGTGAAGGTGCC
	PAX6	Forward	GTG TCT ACC AAC CAA TTC CAC AAC
		Reverse	CCC AAC ATG GAG CCA GAT G
		Probe	CCACACCGGTTTCCTCCTTCACAT
Mesoderm	GATA4	Forward	GAGATGCGTCCCATCAAGAC
		Reverse	ACATCGCACTGACTGAGAAC
		Probe	CTGCTGTGCCCGTAGTGAGATGAC
	TBX3	Forward	CTTTGGGATCAGTTTCACAAGC
		Reverse	CAGCCCAGAACATCTCACTTTA
		Probe	TACCAAGTCGGGAAGGCGAATGTT
	Hand1	Forward	TGAACTCAAGAAGGCGGATG
		Reverse	GGTGCGTCCTTTAATCCTCTT
		Probe	AAACCTTCGTGCTGCTGCAGC

Endoderm	GATA6	Forward	AGACTTGCTCTGGTAATAGCAATA
		Reverse	GAGGCTGTAGGTTGTGTTGT
		Probe	TTCCCATGACTCCAACTTCCACCT
	FOXA2	Forward	CCGACTGGAGCAGCTACTAT
		Reverse	TACGTGTTCATGCCGTTCATC
		Probe	ACTCCTCCGTGAGCAACATGAACG
	EOMES	Forward	CAC CGC CAC CAA ACT GAG AT
		Reverse	CGA ACA CAT TGT AGT GGG CAG
		Probe	AGCTCAAGAAAGGAAACATGCGCC

Table 3. Relative fluorescence intensity (R.F.U) per cell at 96h at MOI (1E6 vg/cell)

iPSC	R.F.U	SEM	**iPSC-RPE**	R.F.U	SEM
AAV3	11.01[a]	± 1.55	AAV6	22.86[a]	± 4.23
AAV7m8	10.19[a]	± 1.35	AAV7m8	17.54[ab]	± 2.91
AAV6	9.20[a]	± 0.91	AAV4	16.33[abc]	± 2.76
AAV2	7.77[a]	± 0.78	AAV3	11.86[bcd]	± 1.90
AAV8	3.18[b]	± 0.40	AAV5	8.82[bcd]	± 1.67
AAV1	2.85[b]	± 0.36	AAV1	8.43[bcd]	± 1.51
AAV9	2.59[b]	± 0.34	AAV2	7.83[cd]	± 1.37
AAV8b	2.30[b]	± 0.30	AAV8	4.68[d]	± 0.95
AAV4	1.43[b]	± 0.42	AAV8b	3.82[d]	± 0.51
AAV7	1.28[b]	± 0.30	AAV7	3.66[d]	± 0.53
AAV5	0.52[b]	± 0.18	AAV9	3.04[d]	± 0.55
Pr > F(Model)	< 0.0001		Pr > F(Model)	< 0.0001	
*SEM: Standard error of mean					

Bibliography:

Ail, D., Perron, M., 2017. Retinal Degeneration and Regeneration—Lessons From Fishes and Amphibians. Curr. Pathobiol. Rep. 5, 67–78. doi:10.1007/s40139-017-0127-9

Aleman, T.S., Han, G., Serrano, L.W., Fuerst, N.M., Charlson, E.S., Pearson, D.J., Chung, D.C., Traband, A., Pan, W., Ying, G.-S., Bennett, J., Maguire, A.M., Morgan, J.I.W.W., 2017. Natural History of the Central Structural Abnormalities in Choroideremia A Prospective Cross-Sectional Study. Ophthalmology 124, 359–373. doi:10.1016/j.ophtha.2016.10.022

Alun R. Barnard, Markus Groppe, and R.E.M., 2015. Gene Therapy for Choroideremia Using an Adeno-Associated Viral (AAV) Vector. Cold Spring Harb Perspect Med 2015;5a017293.

Anand, V., Barral, D.C., Zeng, Y., Brunsmann, F., Maguire, A.M., Seabra, M.C., Bennett, J., 2003. Gene therapy for choroideremia: in vitro rescue mediated by recombinant adenovirus. Vision Res. 43, 919–926. doi:10.1016/S0042-6989(02)00389-9

Atchison, R.W., Casto, B.C., Hammon, W.M., 1965. Adenovirus-associated defective virus particle. Science 149, 754–6. doi:10.1126/science.149.3685.754

Bennett, J., 2017. Taking Stock of Retinal Gene Therapy: Looking Back and Moving Forward. Mol. Ther. 25, 1076–1094. doi:10.1016/j.ymthe.2017.03.008

Berndt, N., Sebti, S.M., 2011. Measurement of protein farnesylation and geranylgeranylation in vitro, in cultured cells and in biopsies, and the effects of prenyl transferase inhibitors. Nat. Protoc. 6, 1775–1791. doi:10.1038/nprot.2011.387

Black, A., Vasireddy, V., Chung, D.C., Maguire, A.M., Gaddameedi, R., Tolmachova, T., Seabra, M., Bennett, J., 2014. Adeno-associated virus 8-mediated gene therapy for choroideremia: preclinical studies in *in vitro* and *in vivo* models. J. Gene Med. 16, 122–130. doi:10.1002/jgm.2768

Blenkinsop, T.A., Saini, J.S., Maminishkis, A., Bharti, K., Wan, Q., Banzon, T., Lotfi, M., Davis, J., Singh, D., Rizzolo, L.J., Miller, S., Temple, S., Stern, J.H., 2015. Human adult retinal pigment epithelial stem cell-derived RPE monolayers exhibit key physiological characteristics of native tissue. Investig. Ophthalmol. Vis. Sci. 56, 7085–7099. doi:10.1167/iovs.14-16246

Bolasco, G., Tracey-White, D.C., Tolmachova, T., Thorley, A.J., Tetley, T.D., Seabra, M.C., Hume, A.N., 2011. Loss of Rab27 function results in abnormal lung epithelium structure in mice. Am. J. Physiol. - Cell Physiol. 300.

Buchholz, D.E., Hikita, S.T., Rowland, T.J., Friedrich, A.M., Hinman, C.R., Johnson, L. V., Clegg, D.O., 2009. Derivation of Functional Retinal Pigmented Epithelium from

Induced Pluripotent Stem Cells. Stem Cells 27, 2427–2434. doi:10.1002/stem.189

Cai, X., Conley, S., Naash, M.I., 2009. RPE65: role in the visual cycle, human retinal disease, and gene therapy. Ophthalmic Genet. 30, 1–9. doi:10.1080/13816810802626399.RPE65

Cereso, N., Pequignot, M.O., Robert, L., Becker, F., De Luca, V., Nabholz, N., Rigau, V., De Vos, J., Hamel, C.P., Kalatzis, V., 2014. Proof of concept for AAV2/5-mediated gene therapy in iPSC-derived retinal pigment epithelium of a choroideremia patient. Mol. Ther. Methods Clin. Dev. 1, 14011. doi:10.1038/mtm.2014.11

Chen, H., 2015. Adeno-associated virus vectors for human gene therapy. World J. Med. Genet. 5, 28. doi:10.5496/wjmg.v5.i3.28

Cremers, F.P.M., Armstrong, S.A., Seabra, M.C., Brown, M.S., Goldstein, J.L., 1994. REP-2, a Rab escort protein encoded by the choroideremia-like gene. J. Biol. Chem. 269, 2111–2117.

Cronin, T., Vandenberghe, L.H., Hantz, P., Juttner, J., Reimann, A., Kacsó, A.-E., Huckfeldt, R.M., Busskamp, V., Kohler, H., Lagali, P.S., Roska, B., Bennett, J., 2014. Efficient transduction and optogenetic stimulation of retinal bipolar cells by a synthetic adeno-associated virus capsid and promoter. EMBO Mol. Med. 6, 1–16. doi:10.15252/emmm.201404077

Dalkara, D., Byrne, L., 2013. In Vivo Directed Evolution of a Novel Adeno- Associated Virus for Therapeutic Outer Retinal Gene Delivery from the Vitreous. Sci. Transl. Med. 5, 1–13.

Deretic, D., 1998. Post-Golgi trafficking of rhodopsin in retinal photoreceptors. Eye 12, 526–530. doi:10.1038/eye.1998.141

Edwards, T.L., Jolly, J.K., Groppe, M., Barnard, A.R., Cottriall, C.L., Tolmachova, T., Black, G.C., Webster, A.R., Lotery, A.J., Holder, G.E., Xue, K., Downes, S.M., Simunovic, M.P., Seabra, M.C., MacLaren, R.E., 2016. Visual Acuity after Retinal Gene Therapy for Choroideremia. N. Engl. J. Med. 374, 1996–1998. doi:10.1056/NEJMc1509501

Ejlerskov, P., Christensen, D.P., Beyaie, D., Burritt, J.B., Paclet, M.-H., Gorlach, A., van Deurs, B., Vilhardt, F., 2012. NADPH Oxidase Is Internalized by Clathrin-coated Pits and Localizes to a Rab27A/B GTPase-regulated Secretory Compartment in Activated Macrophages. J. Biol. Chem. 287, 4835–4852. doi:10.1074/jbc.M111.293696

Esposito, G., De Falco, F., Tinto, N., Testa, F., Vitagliano, L., Tandurella, I.C.M., Iannone, L., Rossi, S., Rinaldi, E., Simonelli, F., Zagari, A., Salvatore, F., 2011. Comprehensive mutation analysis (20 families) of the choroideremia gene reveals a missense variant that prevents the binding of REP1 with rab geranylgeranyl transferase. Hum. Mutat. 32, 1460–1469. doi:10.1002/humu.21591

Freund, P.R., Sergeev, Y. V., MacDonald, I.M., 2016. Analysis of a large choroideremia dataset does not suggest a preference for inclusion of certain genotypes in future trials of gene therapy. Mol. Genet. Genomic Med. 4, 344–358. doi:10.1002/mgg3.208

Ghazi, N.G., Abboud, E.B., Nowilaty, S.R., Alkuraya, H., Alhommadi, A., Cai, H., Hou, R., Deng, W.T., Boye, S.L., Almaghamsi, A., Al Saikhan, F., Al-Dhibi, H., Birch, D., Chung, C., Colak, D., LaVail, M.M., Vollrath, D., Erger, K., Wang, W., Conlon, T., Zhang, K., Hauswirth, W., Alkuraya, F.S., 2016. Treatment of retinitis pigmentosa due to MERTK mutations by ocular subretinal injection of adeno-associated virus gene vector: results of a phase I trial. Hum. Genet. 135, 327–343. doi:10.1007/s00439-016-1637-y

Gibbs, D., Kitamoto, J., Williams, D.S., 2003. Abnormal phagocytosis by retinal pigmented epithelium that lacks myosin VIIa, the Usher syndrome 1B protein. Proc. Natl. Acad. Sci. 100, 6481–6486. doi:10.1073/pnas.1130432100

Gordiyenko, N. V., Fariss, R.N., Zhi, C., MacDonald, I.M., 2010. Silencing of the *CHM* Gene Alters Phagocytic and Secretory Pathways in the Retinal Pigment Epithelium. Investig. Opthalmology Vis. Sci. 51, 1143. doi:10.1167/iovs.09-4117

Heier, J.S., Kherani, S., Desai, S., Dugel, P., Kaushal, S., Cheng, S.H., Delacono, C., Purvis, A., Richards, S., Le-Halpere, A., Connelly, J., Wadsworth, S.C., Varona, R., Buggage, R., Scaria, A., Campochiaro, P.A., 2017. Intravitreous injection of AAV2-sFLT01 in patients with advanced neovascular age-related macular degeneration: a phase 1, open-label trial. Lancet 390, 50–61. doi:10.1016/S0140-6736(17)30979-0

Kamao, H., Mandai, M., Okamoto, S., Sakai, N., Suga, A., Sugita, S., Kiryu, J., Takahashi, M., 2014. Characterization of Human Induced Pluripotent Stem Cell-Derived Retinal Pigment Epithelium Cell Sheets Aiming for Clinical Application. Stem Cell Reports 2, 205–218. doi:10.1016/j.stemcr.2013.12.007

Kern, A., Schmidt, K., Leder, C., Müller, O.J., Wobus, C.E., Lieth, C.W. Von Der, King, J.A., Mu, O.J., Bettinger, K., 2003. Identification of a Heparin-Binding Motif on Adeno-Associated Virus Type 2 Capsids Identification of a Heparin-Binding Motif on Adeno-Associated Virus Type 2 Capsids. J. Virol. 77, 11072–11081. doi:10.1128/JVI.77.20.11072

Koenekoop, R.K., 2007. Choroideremia is Caused by a Defective Phagocytosis by the RPE of Photoreceptor Disc Membranes, not by an Intrinsic Photoreceptor Defect. Ophthalmic Genet. 28, 185–186. doi:10.1080/13816810701407909

Köhnke, M., Delon, C., Hastie, M.L., Nguyen, U.T.T., Wu, Y.-W., Waldmann, H., Goody, R.S., Gorman, J.J., Alexandrov, K., 2013. Rab GTPase Prenylation Hierarchy and Its Potential Role in Choroideremia Disease. PLoS One 8, e81758. doi:10.1371/journal.pone.0081758

Krock, B.L., Bilotta, J., Perkins, B.D., 2007. Noncell-autonomous photoreceptor degeneration in a zebrafish model of choroideremia. Proc. Natl. Acad. Sci. U. S. A.

104, 4600–4605. doi:10.1073/pnas.0605818104

Larijani, B., Hume, A.N., Tarafder, A.K., Seabra, M.C., 2003. Multiple factors contribute to inefficient prenylation of Rab27a in Rab prenylation diseases. J. Biol. Chem. 278, 46798–804. doi:10.1074/jbc.M307799200

Link, B.A., Collery, R.F., 2015. Zebrafish Models of Retinal Disease. Annu. Rev. Vis. Sci. 1, 125–153. doi:10.1146/annurev-vision-082114-035717

MacDonald, I.M., Russell, L., Chan, C.C., 2009. Choroideremia: New Findings from Ocular Pathology and Review of Recent Literature. Surv. Ophthalmol. 54, 401–407. doi:10.1016/j.survophthal.2009.02.008

MacLaren, R.E., Groppe, M., Barnard, A.R., Cottriall, C.L., Tolmachova, T., Seymour, L., Reed Clark, K., During, M.J., Cremers, F.P.M., Black, G.C.M., Lotery, A.J., Downes, S.M., Webster, A.R., Seabra, M.C., 2014. Retinal gene therapy in patients with choroideremia: Initial fi ndings from a phase 1/2 clinical trial. Lancet 383, 1129–1137. doi:10.1016/S0140-6736(13)62117-0

Maguire, A.M., High, K.A., Auricchio, A., Wright, J.F., Pierce, E.A., Testa, F., Mingozzi, F., Bennicelli, J.L., Ying, G. shuang, Rossi, S., Fulton, A., Marshall, K.A., Banfi, S., Chung, D.C., Morgan, J.I., Hauck, B., Zelenaia, O., Zhu, X., Raffini, L., Coppieters, F., De Baere, E., Shindler, K.S., Volpe, N.J., Surace, E.M., Acerra, C., Lyubarsky, A., Redmond, T.M., Stone, E., Sun, J., McDonnell, J.W., Leroy, B.P., Simonelli, F., Bennett, J., 2009. Age-dependent effects of RPE65 gene therapy for Leber's congenital amaurosis: a phase 1 dose-escalation trial. Lancet 374, 1597–1605. doi:10.1016/S0140-6736(09)61836-5

Maguire, A.M., Simonelli, F., Pierce, E.A., Pugh, E.N., Mingozzi, F., Bennicelli, J., Banfi, S., Marshall, K.A., Testa, F., Surace, E.M., Rossi, S., Lyubarsky, A., Arruda, V.R., Konkle, B., Stone, E., Sun, J., Jacobs, J., Dell'Osso, L., Hertle, R., Ma, J., Redmond, T.M., Zhu, X., Hauck, B., Zelenaia, O., Shindler, K.S., Maguire, M.G., Wright, J.F., Volpe, N.J., McDonnell, J.W., Auricchio, A., High, K.A., Bennett, J., 2008. Safety and Efficacy of Gene Transfer for Leber's Congenital Amaurosis. N. Engl. J. Med. 358, 2240–2248. doi:10.1056/NEJMoa0802315

Maguire, J.A., Gagne, A., Mills, J.A., Gadue, P., French, D.L., 2015. Lab resource: Stem cell line Generation of human control iPS cell line CHOPWT9 from healthy adult peripheral blood mononuclear cells. Stem Cell Res. 16, 14–16. doi:10.1016/j.scr.2015.11.005

Mills, J.A., Wang, K., Paluru, P., Ying, L., Lu, L., Galvão, A.M., Xu, D., Yao, Y., Sullivan, S.K., Sullivan, L.M., Mac, H., Omari, A., Jean, J.-C., Shen, S., Gower, A., Spira, A., Mostoslavsky, G., Kotton, D.N., French, D.L., Weiss, M.J., Gadue, P., 2013. Clonal genetic and hematopoietic heterogeneity among human-induced pluripotent stem cell lines. Blood 122.

Moosajee, M., Tulloch, M., Baron, R.A., Gregory-Evans, C.Y., Pereira-Leal, J́. B., Seabra, M.C., 2009. Single choroideremia gene in nonmammalian vertebrates

explains early embryonic lethality of the zebrafish model of choroideremia. Investig. Ophthalmol. Vis. Sci. 50, 3009–3016. doi:10.1167/iovs.08-2755

Moran, N., 2012. First gene therapy approved. Nat. Biotechnol. 30, Preface. doi:10.1038/nbt1212-1153

Murlidharan, G., Samulski, R.J., Asokan, A., 2014. Biology of adeno-associated viral vectors in the central nervous system. Front. Mol. Neurosci. 7, 1–9. doi:10.3389/fnmol.2014.00076

Mustari, M.J., 2017. Nonhuman primate studies to advance vision science and prevent blindness. ILAR J. 58, 216–225. doi:10.1093/ilar/ilx009

Nakano, T., Ando, S., Takata, N., Kawada, M., Muguruma, K., Sekiguchi, K., Saito, K., Yonemura, S., Eiraku, M., Sasai, Y., 2012. Self-formation of optic cups and storable stratified neural retina from human ESCs. Cell Stem Cell 10, 771–785. doi:10.1016/j.stem.2012.05.009

Nightstar Therapeutics, 2018a. Choroideremia [WWW Document].

Nightstar Therapeutics, 2018b. Nightstar Therapeutics Announces Initiation of STAR Phase 3 Registrational Trial for NSR-REP1 in Choroideremia [WWW Document]. URL https://globenewswire.com/news-release/2018/03/05/1414686/0/en/Nightstar-Therapeutics-Announces-Initiation-of-STAR-Phase-3-Registrational-Trial-for-NSR-REP1-in-Choroideremia.html

Parfitt, D.A., Lane, A., Ramsden, C.M., Carr, A.-J.F., Munro, P.M., Jovanovic, K., Schwarz, N., Kanuga, N., Muthiah, M.N., Hull, S., Gallo, J.-M., da Cruz, L., Moore, A.T., Hardcastle, A.J., Coffey, P.J., Cheetham, M.E., 2016. Identification and Correction of Mechanisms Underlying Inherited Blindness in Human iPSC-Derived Optic Cups. Cell Stem Cell 1–13. doi:10.1016/j.stem.2016.03.021

Parfitt, D.A., Lane, A., Ramsden, C.M., Hardcastle, A.J., Coffey, P.J., Cheetham Correspondence, M.E., 2016. Identification and Correction of Mechanisms Underlying Inherited Blindness in Human iPSC- Derived Optic Cups. doi:10.1016/j.stem.2016.03.021

Peng, Y., Tang, L., Zhou, Y., 2017. Subretinal Injection: A Review on the Novel Route of Therapeutic Delivery for Vitreoretinal Diseases. Ophthalmic Res. 58, 217–226. doi:10.1159/000479157

Pillay, S., Meyer, N.L., Puschnik, A.S., Davulcu, O., Diep, J., Ishikawa, Y., Jae, L.T., Wosen, J.E., Nagamine, C.M., Chapman, M.S., Carette, J.E., 2016. An essential receptor for adeno-associated virus infection. Nature 530, 108–112. doi:10.1038/nature16465

Preising, M., Ayuso, C., 2004. Rab escort protein 1 (REP1) in intracellular traffic: a functional and pathophysiological overview. Ophthalmic Genet. 25, 101–110. doi:10.1080/13816810490514333

Preising, M.N., Ayuso, C., 2004. Rab escort protein 1 (REP1) in intracellular traffic: A functional and pathophysiological overview. Ophthalmic Genet. 25, 101–110. doi:10.1080/13816810490514333

Pylypenko, O., Rak, A., Reents, R., Niculae, A., Sidorovitch, V., Cioaca, M.D., Bessolitsyna, E., Thomä, N.H., Waldmann, H., Schlichting, I., Goody, R.S., Alexandrov, K., 2003. Structure of Rab escort protein-1 in complex with Rab geranylgeranyltransferase. Mol. Cell 11, 483–494. doi:10.1016/S1097-2765(03)00044-3

Radziwon, A., Arno, G., K. Wheaton, D., McDonagh, E.M., Baple, E.L., Webb-Jones, K., G. Birch, D., Webster, A.R., MacDonald, I.M., 2017. Single-base substitutions in the CHM promoter as a cause of choroideremia. Hum. Mutat. 38, 704–715. doi:10.1002/humu.23212

Rak, A., Pylypenko, O., Niculae, A., Pyatkov, K., Goody, R.S., Alexandrov, K., 2004. Structure of the Rab7:REP-1 complex: Insights into the mechanism of Rab prenylation and choroideremia disease. Cell 117, 749–760. doi:10.1016/j.cell.2004.05.017

Ramachandran, P.S., Lee, V., Wei, Z., Song, J.Y., Casal, G., Cronin, T., Willett, K., Huckfeldt, R., Morgan, J.I.W., Aleman, T.S., Maguire, A.M., Bennett, J., 2017. Evaluation of Dose and Safety of AAV7m8 and AAV8BP2 in the Non-Human Primate Retina. Hum. Gene Ther. 28, 154–167. doi:10.1089/hum.2016.111

Rapti, K., Stillitano, F., Karakikes, I., Nonnenmacher, M., Weber, T., Hulot, J.S., Hajjar, R.J., 2015. Effectiveness of gene delivery systems for pluripotent and differentiated cells. Mol. Ther. - Methods Clin. Dev. 2, 1–14. doi:10.1038/mtm.2014.67

Russell, S., Bennett, J., Wellman, J.A., Chung, D.C., Yu, Z.F., Tillman, A., Wittes, J., Pappas, J., Elci, O., McCague, S., Cross, D., Marshall, K.A., Walshire, J., Kehoe, T.L., Reichert, H., Davis, M., Raffini, L., George, L.A., Hudson, F.P., Dingfield, L., Zhu, X., Haller, J.A., Sohn, E.H., Mahajan, V.B., Pfeifer, W., Weckmann, M., Johnson, C., Gewaily, D., Drack, A., Stone, E., Wachtel, K., Simonelli, F., Leroy, B.P., Wright, J.F., High, K.A., Maguire, A.M., 2017. Efficacy and safety of voretigene neparvovec (AAV2-hRPE65v2) in patients with RPE65-mediated inherited retinal dystrophy: a randomised, controlled, open-label, phase 3 trial. Lancet 390, 849–860. doi:10.1016/S0140-6736(17)31868-8

Sanchez-Alcudia, R., Garcia-Hoyos, M., Lopez-Martinez, M.A., Sanchez-Bolivar, N., Zurita, O., Gimenez, A., Villaverde, C., Rodrigues-Jacy, L., Silva, D., Corton, M., Perez-Carro, R., Torriano, S., Kalatzis, V., Rivolta, C., Avila-Fernandez, A., Lorda, I., Trujillo-Tiebas, M.J., Garcia-Sandoval, B., Lopez-Molina, M.I., Blanco-Kelly, F., Riveiro-Alvarez, R., Ayuso, C., Sanchez-Alcudia, R., -Hoyos, G., Ma, L.-M., Sanchez-Bolivar, N., Zurita, O., Gimenez, A., Janecke, A.R., 2016. A Comprehensive Analysis of Choroideremia: From Genetic Characterization to Clinical Practice. PLoS One 11. doi:10.1371/journal.pone.0151943

Schnabolk, G., Parsons, N., Obert, E., Annamalai, B., Nasarre, C., Tomlinson, S., Lewin,

A.S., Rohrer, B., 2018. Delivery of CR2-fH Using AAV Vector Therapy as Treatment Strategy in the Mouse Model of Choroidal Neovascularization. Mol. Ther. - Methods Clin. Dev. 9, 1–11. doi:10.1016/j.omtm.2017.11.003

Seabra, M.C., Brown, M.S., Slaughter, C.A., Südhof, T.C., Goldstein, J.L., 1992. Purification of component A of Rab geranylgeranyl transferase: Possible identity with the choroideremia gene product. Cell 70, 1049–1057. doi:10.1016/0092-8674(92)90253-9

Seabra, M.C., Ho, Y.K., Anant, J.S., 1995. Deficient Geranylgeranylation of Ram / Rab27 in Choroideremia. J. Biol. Chem. 270, 24420–24427. doi:10.1074/jbc.270.41.24420

Sergeev, Y. V., Smaoui, N., Sui, R., Stiles, D., Gordiyenko, N., Strunnikova, N., MacDonald, I.M., 2009. The functional effect of pathogenic mutations in Rab escort protein 1. Mutat. Res. - Fundam. Mol. Mech. Mutagen. 665, 44–50. doi:10.1016/j.mrfmmm.2009.02.015

Siemiatkowska, A.M., Collin, R.W.J., Den Hollander, A.I., Cremers, F.P.M., 2014. Genomic approaches for the discovery of genes mutated in inherited retinal degeneration. Cold Spring Harb. Perspect. Med. 4, 1–14. doi:10.1101/cshperspect.a017137

Silène T. Wavre-Shapton, Tolmachova, T., Lopes Da Silva, M., Futter, C.E., Seabra, M.C., 2013. Conditional Ablation of the Choroideremia Gene Causes Age-Related Changes in Mouse Retinal Pigment Epithelium. PLoS One 8. doi:10.1371/journal.pone.0057769

Simó, R., Villarroel, M., Corraliza, L., Hernández, C., Garcia-Ramírez, M., 2010. The retinal pigment epithelium: Something more than a constituent of the blood-retinal barrier-implications for the pathogenesis of diabetic retinopathy. J. Biomed. Biotechnol. 2010. doi:10.1155/2010/190724

Simunovic, M.P., Jolly, J.K., Xue, K., Edwards, T.L., Groppe, M., Downes, S.M., MacLaren, R.E., 2016. The Spectrum of CHM Gene Mutations in Choroideremia and Their Relationship to Clinical Phenotype. Investig. Opthalmology Vis. Sci. 57, 6033. doi:10.1167/iovs.16-20230

Sonoda, S., Spee, C., Barron, E., Ryan, S.J., Kannan, R., Hinton, D.R., 2009. A protocol for the culture and differentiation of highly polarized human retinal pigment epithelial cells. Nat. Protoc. 4, 662–673. doi:10.1038/nprot.2009.33

Spark Therapeutics, 2018. Choroideremia Phase 1/2 clinical trial SPK-7001 [WWW Document]. URL http://sparktx.com/scientific-platform-programs/

Sparrow, J.R., Hicks, D., Hamel, C.P., 2010. The retinal pigment epithelium in health and disease. Curr. Mol. Med. 10, 802–23. doi:10.1016/j.biotechadv.2011.08.021.Secreted

Strauss, O., 2005. The Retinal Pigment Epithelium in Visual Function. Physiol. Rev. 85, 845–881. doi:10.1152/physrev.00021.2004.

Strunnikova, N., Zein, W.M., Silvin, C., MacDonald, I.M., 2012. Serum Biomarkers and Trafficking Defects in Peripheral Tissues Reflect the Severity of Retinopathy in Three Brothers Affected by Choroideremia. Springer, Boston, MA, pp. 381–387. doi:10.1007/978-1-4614-0631-0_49

Strunnikova, N. V, Barb, J., Sergeev, Y. V, Thiagarajasubramanian, A., Silvin, C., Munson, P.J., Macdonald, I.M., 2009. Loss-of-Function Mutations in Rab Escort Protein 1 (REP-1) Affect Intracellular Transport in Fibroblasts and Monocytes of Choroideremia Patients. doi:10.1371/journal.pone.0008402

Sullivan, S.K., Mills, J.A., Koukouritaki, S.B., Vo, K.K., Lyde, R.B., Paluru, P., Zhao, G., Zhai, L., Sullivan, L.M., Wang, Y., Kishore, S., Gharaibeh, E.Z., Lambert, M.P., Wilcox, D.A., French, D.L., Poncz, M., Gadue, P., 2014. High-level transgene expression in induced pluripotent stem cell-derived megakaryocytes: correction of Glanzmann thrombasthenia. Blood 123, 753–7. doi:10.1182/blood-2013-10-530725

Summerford, C., Samulski, R.J., 2016. AAVR: A multi-serotype receptor for AAV. Mol. Ther. 24, 663–666. doi:10.1038/mt.2016.49

Sun, L.W., Johnson, R.D., Williams, V., Summerfelt, P., Dubra, A., Weinberg, D. V., Stepien, K.E., Fishman, G.A., Carroll, J., 2016. Multimodal imaging of photoreceptor structure in Choroideremia. PLoS One 11. doi:10.1371/journal.pone.0167526

Tolmachova, T., Tolmachov, O.E., Barnard, A.R., De Silva, S.R., Lipinski, D.M., Walker, N.J., Maclaren, R.E., Seabra, M.C., 2013. Functional expression of Rab escort protein 1 following AAV2-mediated gene delivery in the retina of choroideremia mice and human cells ex vivo.

Tolmachova, T., Tolmachov, O.E., Wavre-Shapton, S.T., Tracey-White, D., Futter, C.E., Seabra, M.C., 2012. CHM/REP1 cDNA delivery by lentiviral vectors provides functional expression of the transgene in the retinal pigment epithelium of choroideremia mice. J. Gene Med. 14, 158–168. doi:10.1002/jgm.1652

Tolmachova, T., Wavre-Shapton, S.T., Barnard, A.R., MacLaren, R.E., Futter, C.E., Seabra, M.C., 2010. Retinal pigment epithelium defects accelerate photoreceptor degeneration in cell type-specific knockout mouse models of choroideremia. Investig. Ophthalmol. Vis. Sci. 51, 4913–4920. doi:10.1167/iovs.09-4892

Uchholz, D.A.E.B., Ennington, B.R.O.P., Roze, R.O.H.C., 2013. Rapid and Efficient Directed Differentiation of Human Pluripotent Stem Cells Into Retinal Pigmented Epithelium 384–393.

Van den Hurk, J.A.J.M., Hendriks, W., Van de Pol, D.J.R., Oerlemans, F., Jaissle, G., Ruther, K., Kohler, K., Hartmann, J., Zrenner, E., Van Bokhoven, H., Wieringa, B., Ropers, H.H., Cremers, F.P.M., 1997. Mouse chorioderemia gene mutation causes

photoreceptor cell degeneration and is not transmitted through the female germline. Hum. Mol. Genet. 6, 851–858.

Vance, M.A., Mitchell, A., Samulski, R.J., 2015. AAV Biology , Infectivity and Therapeutic Use from Bench to Clinic. InTech. doi:http://dx.doi.org/10.5772/61988

Vandenberghe, L.H., Bell, P., Maguire, A.M., Cearley, C.N., Xiao, R., Calcedo, R., Wang, L., Castle, M.J., Maguire, A.C., Grant, R., Wolfe, J.H., Wilson, J.M., Bennett, J., 2011. Dosage thresholds for AAV2 and AAV8 photoreceptor gene therapy in monkey. Sci. Transl. Med. 3. doi:10.1126/scitranslmed.3002103

Vasireddy, V., Mills, J.A., Gaddameedi, R., Basner-Tschakarjan, E., Kohnke, M., Black, A.D., Alexandrov, K., Zhou, S., Maguire, A.M., Chung, D.C., Mac, H., Sullivan, L., Gadue, P., Bennicelli, J.L., French, D.L., Bennett, J., Kirby, F.M., 2013. AAV-Mediated Gene Therapy for Choroideremia: Preclinical Studies in Personalized Models. PLoS One 8. doi:10.1371/journal.pone.0061396

Veleri, S., Lazar, C.H., Chang, B., Sieving, P.A., Banin, E., Swaroop, A., 2015. Biology and therapy of inherited retinal degenerative disease: insights from mouse models. Dis. Model. Mech. 8, 109–129. doi:10.1242/dmm.017913

Vugler, A., Carr, A.J., Lawrence, J., Chen, L.L., Burrell, K., Wright, A., Lundh, P., Semo, M., Ahmado, A., Gias, C., da Cruz, L., Moore, H., Andrews, P., Walsh, J., Coffey, P., 2008. Elucidating the phenomenon of HESC-derived RPE: Anatomy of cell genesis, expansion and retinal transplantation. Exp. Neurol. 214, 347–361. doi:10.1016/j.expneurol.2008.09.007

Yamaoka, M., Ando, T., Terabayashi, T., Okamoto, M., Takei, M., Nishioka, T., Kaibuchi, K., Matsunaga, K., Ishizaki, R., Izumi, T., Niki, I., Ishizaki, T., Kimura, T., 2016. PI3K regulates endocytosis after insulin secretion by mediating signaling crosstalk between Arf6 and Rab27a. J. Cell Sci. 129, 637–649. doi:10.1242/jcs.180141

Zhang, A.Y., Mysore, N., Vali, H., Koenekoop, J., Cao, S.N., Li, S., Ren, H., Keser, V., Lopez-Solache, I., Siddiqui, S.N., Khan, A., Mui, J., Sears, K., Dixon, J., Schwartzentruber, J., Majewski, J., Braverman, N., Koenekoop, R.K., 2015a. Choroideremia is a systemic disease with lymphocyte crystals and plasma lipid and RBC membrane abnormalities. Investig. Ophthalmol. Vis. Sci. 56, 8158–8165. doi:10.1167/iovs.14-15751

Zhang, A.Y., Mysore, N., Vali, H., Koenekoop, J., Cao, S.N., Li, S., Ren, H., Keser, V., Lopez-Solache, I., Siddiqui, S.N., Khan, A., Mui, J., Sears, K., Dixon, J., Schwartzentruber, J., Majewski, J., Braverman, N., Koenekoop, R.K., 2015b. Choroideremia Is a Systemic Disease With Lymphocyte Crystals and Plasma Lipid and RBC Membrane Abnormalities. Investig. Opthalmology Vis. Sci. 56, 8158. doi:10.1167/iovs.14-15751

Zhang, Z., Zhang, Y., Xiao, H., Liang, X., Sun, D., Peng, S., 2012. A gene expression profile of the developing human retinal pigment epithelium. Mol. Vis. 18, 2961–75.

Zhong, X., Gutierrez, C., Xue, T., Hampton, C., Vergara, M.N., Cao, L.-H., Peters, A., Park, T.S., Zambidis, E.T., Meyer, J.S., Gamm, D.M., Yau, K.-W., Canto-Soler, M.V., 2014. Generation of three-dimensional retinal tissue with functional photoreceptors from human iPSCs. Nat. Commun. 5, 4047. doi:10.1038/ncomms5047